v. 4, n. 27, 2024

Journal of Engineering Research

Acceptance date: 28/11/2024

STUDY OF EEG SIGNALS USING THE WAVELET TRANSFORM TO IDENTIFY ADHD IN SCHOOL-AGE CHILDREN

Amanda Brito Oliveira da Silva
Biomedical Engineering, Universidade Federal do Rio Grande do Norte (UFRN)

Alice Barros da Silva
Biomedical Engineering, Universidade Federal do Rio Grande do Norte (UFRN)

Ana Luiza Ohara de Queiroz
Biomedical Engineering, Universidade Federal do Rio Grande do Norte (UFRN)

Lucas Jácomo Bueno
Biomedical Engineering, Universidade Federal do Rio Grande do Norte (UFRN)

Manuelly Gomes Da Silva
Biomedical Engineering, Universidade Federal do Rio Grande do Norte (UFRN)

Maria Eduarda Varela Barbosa
Biomedical Engineering, Universidade Federal do Rio Grande do Norte (UFRN)

Mariana Fernandes Dourado Pinto
Biomedical Engineering, Universidade Federal do Rio Grande do Norte (UFRN)

Nadyne Dayonara Maurício de Amorim
Biomedical Engineering, Universidade Federal do Rio Grande do Norte (UFRN)

Nícolas Vinícius Rodrigues Veras
Biomedical Engineering, Universidade Federal do Rio Grande do Norte (UFRN)

Samara Dália Tavares Silva
Biomedical Engineering, Universidade Federal do Rio Grande do Norte (UFRN)

Custódio Leopoldino de Brito Guerra Neto
Professor of Biomedical Engineering at the Universidade Federal do Rio Grande do Norte (UFRN)

Ernano Arrais Junior
Biomedical Engineering, Universidade Federal do Rio Grande do Norte (UFRN)

Abstract: Attention Deficit/Hyperactivity Disorder (ADHD) is a neurobiological disorder characterized by a persistent pattern of inattention/hyperactivity-impulsivity. In school-age children, the influence of this disorder can lead to low academic performance, but the main factor is the interference in the individual's social, academic and professional life. Therefore, this study aims to develop an analysis system based on the Electroencephalogram (EEG) signal to encourage the development of tools to identify signs suggestive of ADHD in school children. To this end, the classifier is based on the *Threshold* technique using the Redundant Discrete Wavelet Transform to extract signal characteristics. The simulation environment used was MATLAB (2015a). The data set analyzed was from the *IEEE Dataport* database. To achieve the objective of the work, the delta and theta frequency ranges of the *wavelet* coefficients were used as parameters for the *threshold* method, and the electrodes analyzed were from the frontal region of the brain. The proposed model performed with a sensitivity of 88.58 % and positive predictivity of 73.26 % for a set of 40 analyzed data. Among the aspects identified, it can be seen that the algorithm's performance was satisfactory, however, for a small volume of data.
Keywords: Electroencephalography. Wavelet transform. ADHD.

INTRODUCTION

Attention-Deficit/Hyperactivity Disorder (ADHD), according to the Diagnostic and Statistical Manual of Mental Disorders 5th edition (DSM-5), is a neurodevelopmental disorder characterized by a persistent pattern of inattention and/or hyperactivity-impulsivity that interferes with the individual's development (American Psychiatric Association, 2014).

Thus, some symptoms of ADHD may involve: inattention to detail, difficulty maintaining concentration when carrying out activities, as well as difficulty organizing tasks. In addition, there is the possibility of hyperactivity and impulsivity with agitation and hyperactivity of motor activity, such as: frequently getting up from the chair, squirming in the chair, difficulty listening to others or interrupting others' speech, among other possible symptoms (American Psychiatric Association, 2014).

For a clinical diagnosis, most of the symptoms must be present, even if in different forms, with a substantial presence of symptoms before the age of 12. In addition, the symptoms must interfere with the functioning of the individual's social, academic and professional life (American Psychiatric Association, 2014).

The worldwide prevalence of ADHD in children and adolescents is between 3% and 8%. In Brazil, it is around 7.6% in children and adolescents aged between 6 and 17 and 5.2% in people aged between 18 and 44 (BRASIL, 2022). The Brazilian Attention Deficit Disorder Association (ABDA) also reports that the disorder in children ranges from 3% to 5% of the child population (ABDA, 2016).

The risk factors for ADHD include environmental, genetic and physiological factors. In this context, the possible consequences of the disorder can be: low academic performance, emotional and behavioral problems. Although the presence of ADHD does not mean interference in the child's life (American Psychiatric Association, 2014).

In this context, the exploratory field study by Couras et al. (2018) aimed to identify the prevalence of ADHD characteristics with a quantitative approach. In this way, the group assessed were students in the second year of elementary school in public schools in the Sertão Paraibano. The descriptive research found that 50.35% of the 95 students assessed had some symptom of the disorder, and among the 50.35%, 12.35% had hyperactivity and 19% inattention, 19% hyperactivity and inattention. Thus, it is clear that the study is relevant in exploring the presence of the disorder among children and adolescents since the result was significant for the possibility of signs suggestive of ADHD, in addition, the study emphasizes the lack of information on the part of the community, family and school, about ADHD.

ADHD is a neurodevelopmental disorder that involves clinical diagnosis. Thus, investigating the variation of electroencephalogram (EEG) signals in patients with ADHD presents an advantageous way of exploring the singularities of the disorder. Thus, the results of the literature review by Slater et al (2022) show that there is significant information on the EEG signal that makes ADHD symptomatology promising, although there is no definitive biological marker that is diagnostic of ADHD. The study points to the differentiation of subtypes and symptoms of the disorder in the resting state and modulation related to the alpha, beta and theta power task, among others. From this, it is possible to indicate that the correlation between ADHD and the EEG signal points to promising research into the disorder.

In order to understand the behavior of brain activity, EEG technology is used to record electrical signals from the brain (TATUM et al., 2008). It is a non-invasive method that allows a graphic display of the difference in voltage between two recording sites over time. The types of activity recorded by the EEG include morphology, frequency, amplitude, rhythmicity, symmetry, synchrony and reactivity (MORCH et al., 2021).

Among the mathematical tools used to analyze biological signals is the Wavelet Transform (WT) method, which allows data to be analyzed at various scales and resolutions,

both globally and in terms of signal details in the time and frequency domain (BARBOSA et.al, 2008).

Arrais Junior (2016) used the Discrete Wavelet Transform Redundant (TWDR) technique from the *Daubechies* family and the *Daubechies* 4 (db4) mother *wavelet* to analyze electrocardiogram signals. The paper presented a system for analyzing electrocardiogram signals in real time using *thresholding* techniques. The system achieved sensitivity of 99.20% and positive predictivity of 99.64%.

Cortés (2021) in his final paper presented a classifier for ADHD using the Discrete Wavelet Transform (DWT) with the *Daubechies* family and the db4 mother *wavelet*, due to the identification of singular characteristics in electrophysiological signals. In addition, the technique used to study the possible presence of ADHD was logistic regression. The classifier's performance was 96 % for cross-validation, for a study group of 64 children

Thus, given the importance of characterizing ADHD in the elementary school environment in public schools, this study seeks to explore EEG data from children with ADHD, as a strategy to substantiate the clinical diagnosis to identify signs related to ADHD using the Redundant Discrete Wavelet Transform (RDWT) and the *threshold* technique, based on the *Daubechies* family *and* the db4 mother *wavelet*, evaluating the delta and theta *wave of the wavelet* coefficients of the electrodes in the frontal region.

RELEVANCE

The field of study involving EEG and ADHD in order to identify a diagnostic biomarker for the disorder has been studied by researchers over the years. Although there is no definitive biological marker that is diagnostic of ADHD**.** Given the lack of knowledge in this area, the research by Slater *et al.* (2022) pointed to significant results in ADHD symptomatology. In addition, the tools used have unstable prediction accuracy (CHEN *et al.*, 2019). In view of this, this work seeks to make an exploratory contribution to the identification of signs related to ADHD.

MOTIVATION

The motivation for the project arose from the questioning of the impact of ADHD in the school environment. The study by Pedroso et al. carried out exploratory and descriptive research to investigate the presence of classroom resources to assist students with ADHD in the school environment. The study was carried out in the municipality of Uruguaiana, in Rio Grande do Sul, in two public primary schools. Of the 44 teachers, only 17 answered the questionnaire. The results show that 41.18% of teachers believe that the model partially guarantees inclusion, 23.53% of teachers believe that it does not guarantee inclusion, 35.29% fully guarantees inclusion and 5.88% have no information about the presence of resources for students with ADHD. In this way, the survey demonstrates the deficiency in the structure of the school environment to meet the possible needs of the student in the classroom.

Furthermore, recent research points to a high prevalence rate of ADHD in children and adolescents. As a result, a public school in Salvador in the state of Bahia evaluated a group of 265 elementary school students who presented clinical signs of ADHD. The result obtained was that 16.6% of the students presented symptoms of ADHD (OLIVEIRA et al., 2022). Thus, the result indicates that there is a prevalence of the disorder in the school environment. Thus, educational policies that discuss ADHD are necessary in the school environment to disseminate knowledge about ADHD.

OBJECTIVES

GENERAL

The aim of this work is to develop a system for evaluating EEG signals that may be related to ADHD in children, using the Wavelet Transform and *Threshold* techniques.

SPECIFIC

To achieve the general objective, the following specific objectives were set.

- Collect and identify the biological signal of children with ADHD and without ADHD from the *IEEE Dataport* database;
- Analyze the EEG signal in children with ADHD and without ADHD;
- Understanding and applying the Redundant Discrete Wavelet Transform;
- Perform signal analysis;
- Extract information from *wavelet* coefficients;
- Create a classifier with the *wavelet* coefficients (W4, W5 and W6);
- Perform tests with the classifier.

CONTRIBUTIONS

The proposal of this work contributes to an initial screening of possible EEG alterations suggestive of ADHD, given that there is no definitive biomarker for ADHD. But it can substantiate the diagnosis of ADHD in school-age children. It makes it possible to analyze EEG signals, as well as identifying them so that the child or adolescent can later be referred to a health service.

METHODOLOGY

The organization of the proposed research will follow these steps:

Initially, the set of 40 EEG signal data from children with and without ADHD were downloaded from the *IEEE Dataport* database. The data was then analyzed using the TWDR mathematical tool in the MATLAB (2015a) simulation environment to extract signal characteristics, which will return information on: approximation coefficients, *wavelet* coefficients and energy at 6 levels of resolution.

In the second stage, the singularities of the results obtained in the previous stage are analyzed and understood for the two sets of children with and without ADHD. Subsequently, the *wavelet* coefficients of the 4,5 and 6 scale are used as parameters for the *thresholding* technique.

Finally, the *threshold* method with the *wavelet* coefficients of the 4,5 and 6 scale is used to identify signs suggestive of ADHD.

WORK ORGANIZATION

This paper is divided into the following sections.

Chapter 1 begins with an introduction to ADHD, presenting information from the DSM-5, statistical data, as well as a general contextualization of the work on EEG and the TWDR technique.

Chapter 2 reviews the literature on ADHD and the use of EEG as a detection tool for the disorder, as well as mathematical tools used in research to detect ADHD.

Chapter 3 presents the EEG technique for recording brain activity, discussing how the procedure works. Chapter 4 presents the tool used in this work, the TWDR, discussing the mathematical equations of the mechanism, as well as the advantages of the technique.

Chapter 5 shows the signal classification method for identifying ADHD-related signals, in which the classification logic is dis-

cussed in detail. The results and discussions are presented in Chapter 6. These include the results obtained from the TWDR mathematical tool, as well as the performance of the classifier.

Finally, Chapter 6 presents the conclusions of this work, as well as suggestions for future work.

LITERATURE REVIEW

EEG SIGNAL WITH EMPHASIS ON ATTENTION DEFICIT HYPERACTIVITY DISORDER

In recent years, the rate of ADHD has risen sharply in Brazil and around the world, arousing the interest of several authors in the search for biomarkers that can help in the clinical diagnosis of the disorder. Some of the studies carried out include:

Markovska-Simoska and Pop-Jordanova (2016) evaluated the absolute and relative power of the EEG and verified the theta and beta relationship in individuals with ADHD. The observations made were that children with ADHD had an increase in the absolute power of the delta and theta waves, which is not seen in adults with the disorder. There was also greater relative power in theta and beta waves in children with ADHD.

Giertuga et al. (2017) studied age-related changes using EEG in 74 healthy children and 67 diagnosed with ADHD in a resting state. From this, it was observed that the ADHD group had a lower absolute power in relation to the theta band compared to the healthy group.

Ibrahim et al. (2019) also aimed to detect EEG abnormalities in children with ADHD. Thus, the study group consisted of 60 healthy children and 60 with ADHD, the conclusion of the study found that there was an increase in low-frequency bands and a decrease in high-frequency activity for children with ADHD.

Ekhlasi et al. (2021) studied the information pathways of brain activity in 61 children with and 60 without ADHD using EEG information during a visual activity. The detection parameter was the calculation of directed phase transfer entropy in the delta, theta, alpha, beta and lower gamma frequency bands. The results obtained were in the beta band with a greater flow of information in the anterior region for the control group. In contrast, a difference was observed in the delta band for individuals with ADHD.

MATHEMATICAL TOOLS FOR ANALYZING ATTENTION DEFICIT HYPERACTIVITY DISORDER

Studies on EEG signals for individuals with ADHD have been explored in recent years, with the aim of finding a biomarker indicative of ADHD. With this in mind, mathematical tools are being applied to EEG signal processing in order to extract characteristics and classify the ADHD EEG signal.

Mohammadi et al. (2016), proposed a model to detect children with ADHD and children without the disorder using EEG when performing activities. To this end, the techniques of approximate entropy, *Iyapunov* exponent and fractal dimension were used to capture signal characteristics, in addition to the *Double Input Symmetrical Relevance* (DISR) and *Minimum Redundancy Maximum Relevance* (mRMR) relevance methods to improve the neural network's classification result. The results obtained were 92.28 % accuracy using mRMR and 93.65 % with DISR in the *Multi-Layer Perceptron* (MLP) *Neural Network* (NN).

Allahverdy A. et al. (2016) also used NN *Multi-Layer Perceptron* as a classifier to identify children with ADHD. The following methods were applied to verify the uniqueness of the EEG signal: *Lyapunov*'s exponent, *Higuchi*'s fractal dimension, *Katz*'s fractal dimen-

sion and *Sevcik*'s fractal dimension to assess the patients' attention state. The result was that the frontal lobe region showed the best accuracy at 96.7%, showing that there is a disparity between children with and without ADHD.

Dubreuil-Vall, Ruffini and Camprodon (2020) also used a four-layer CNN with clustering and filtering, using spectrograms related to EEG events to differentiate ADHD from healthy individuals. The result of the classifier was approximately 88%.

Taghibeyglou et al. (2022), use the *Convolutional Neural Network* (CNN) structure to classify the ADHD condition. It also uses support vector machine, logistic regression and random forest techniques, among others, to extract features from the raw EEG signal. Finally, the proposal achieved approximately 86.33% accuracy without using mapping. However, for the condition of specific selection of classifiers, the accuracy achieved was around 91.16 %.

Finally, Table 1 shows a summary table of the aforementioned techniques. It shows the metrics used to analyze the algorithm and the results obtained. The parameters used differ between the authors' techniques, however, the performances obtained prove to be satisfactory in the exploratory study of EEG signals suggestive of ADHD.

ELECTROENCEPHALOGRAM

The electroencephalogram allows the electrical signals of the brain to be recorded. The recording of brain activity can be extracranial, in which the electrodes are positioned on the surface of the scalp, being a non-invasive method, as well as allowing a graphic display of the difference in voltages of two recording sites over time from both hemispheres of the brain. Another method is intracranial, where electrodes are surgically implanted to provide a specific recording of the brain region (TATUM et al., 2008). The recorded characteristics of the EEG signal include morphology, frequency, amplitude, rhythmicity, symmetry, synchrony and reactivity (MORCH et al., 2021). In this way, recording the EEG signal makes it possible to detect diseases at an early stage (SANEI; CHAMBERS, 2007). It also allows neurological disorders to be detected from the behavior of the EEG signal (ALTURKI *et al.*, 2020).

BASIC PHYSIOLOGY OF BRAIN POTENTIALS

The electrical signals that occur in the brain are created by electrical charges that flow into the Central Nervous System (CNS) (TATUM et al., 2008). The CNS is made up of nerve cells, also called neurons, and glial cells. The response to stimuli and the transmission of information occurs through nerve cells. Likewise, the transmission of the electrical impulse occurs through the axon, which is connected to other dendrites that receive the electrical impulse and relay the signal to other nerves. The propagation of information between axons and dendrites or dendrites and dendrites of cells is called a synapse. Figure 1 shows the components of the neuron's structure that cooperate to propagate the nerve impulse (SANEI; CHAMBERS, 2007).

The Action Potential (AP) is the information transmitted along a nerve through the exchange of ions in the neuron's membrane. For an action potential to occur, the stimulus must reach a level higher than the activation threshold. Stimuli can be: chemical, electrical, luminous, among others (SANEI; CHAMBERS, 2007). In Figure 1, the AP begins when the activation threshold is reached, when the cell depolarizes and sodium (Na+) channels open, when ions enter the cell. At the peak of the signal, the Na+ channels close and the potassium (K+)-dependent channels open, re-

REFERENCE	TECHNICAL	PARAMETER	RESULT
Mohammadi et al. (2016)	DISR and mRMR	precision	92,28 % e 93,65 %
Nasrabadi et al.(2016)	NN	accuracy	96,7 %
Taghibeyglou et al. (2022)	CNN	precision	86,33 %
Dubreuil-Vall, Ruffini and Camprodon (2020)	CNN	precision	88 %
Cortés (2021)	TWD	cross-validation	96 %

Table 1: Summary table of the techniques used to analyze the ADHD EEG signal.

Source: Prepared by the author (2022).

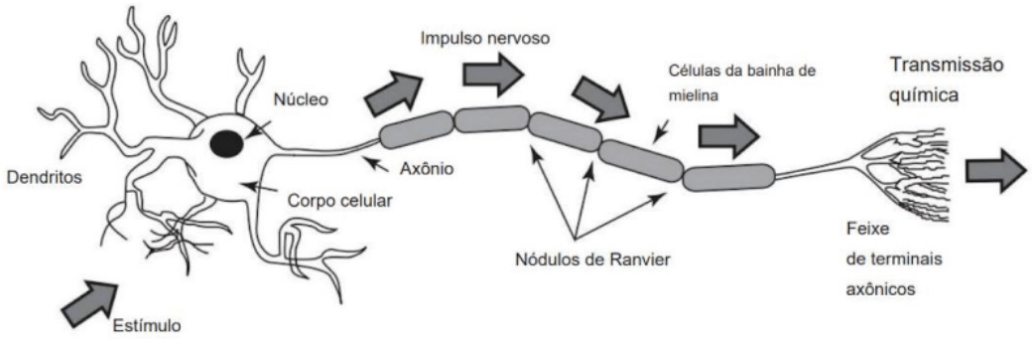

Figure 1: Illustrative image of the structure of a neuron.

Source: Sanei; Chambers (2007)

polarizing the cell. Before reaching the resting potential, the cell hyperpolarizes, preventing it from receiving another stimulus (SANEI; CHAMBERS, 2007).

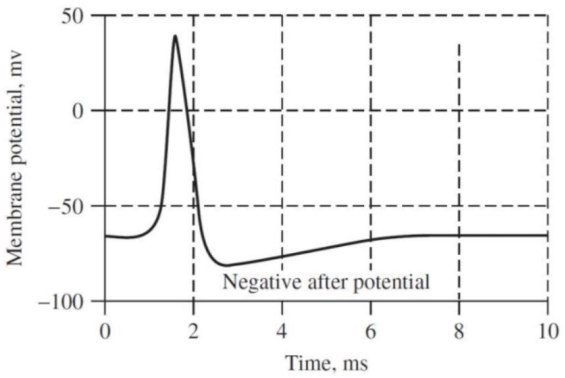

Figure 2: Action potential.

Source: Sanei; Chambers (2007)

EEG SIGNAL ACQUISITION

The capture of the EEG signal follows the standard of the International Federation of Societies of Electroencephalography and Clinical Neurophysiology, with the terminology "10-20". This represents the standard measurement interval of 10% or 20% (LOUIS et al., 2016). Standardization refers to the positioning of the electrodes on the scalp. This electrode placement region is subdivided into 10% and 20% intervals (TATUM et al., 2008). This conventional configuration is for 21 electrodes, with the exception of the left and right earlobe electrodes, represented by A1 and A2 respectively, which are used as reference electrodes. Therefore, the term "10 or 20%" refers to the distance between the electrodes (SANEI; CHAMBERS, 2007). Figure 3 shows the distribution of the electrodes according to the 10%-20% standard.

The positioning of the electrodes, according to the "10-20" standard, favors complete coverage of the entire scalp. It is guided by the positioning of the bones and

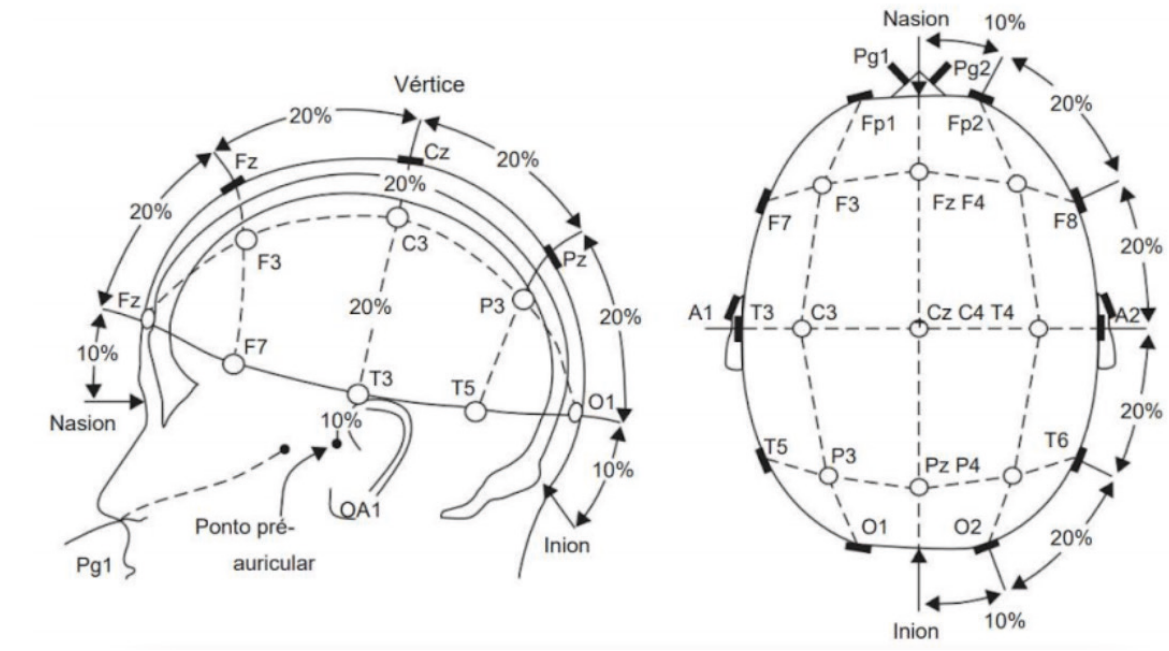

Figure 3: Representation of the 10-20 EEG pattern.

Source: Sanei; Chambers (2007)

their distances. The regions of the brain are indicated by numerical indices and letters (SANEI; CHAMBERS, 2007).

- Earpiece - A;
- Central- C;
- Parietal - P;
- Front - F;
- Polar Front - F;
- Occipital - O;
- Temporal - T.

In a nutshell, signal acquisition begins with the capture of the electrical potential by the electrodes located on the surface of the scalp and then conducted to the electrode box, called the *jack box*. Next, an assembly selector allows the EEG signal to be amplified and finally the signal is filtered (TATUM et al., 2008).

BRAIN RHYTHM

The EEG signal enables the diagnosis of a brain disorder. Clinical specialists therefore analyze the brain rhythms of EEG signals as a parameter for identification. The EEG signal changes from individual to individual, with alterations in the amplitude and frequency of the signal, and age is also a factor in altering the behavior of the EEG signal. The literature segments the frequency bands into 5 ranges (SANEI; CHAMBERS, 2007).

- Delta waves (δ) in the range of 0.5 to 4 Hz;
- Theta waves (θ) in the 4 to 7.5 Hz range;
- Alpha waves (α) in the 8 to 13 Hz range;
- Beta waves (β) in the 14 to 26 Hz range;
- Gamma waves (γ)) above 30 Hz.

In this way, the signal can be broken down into a series of sine waves to form the frequency spectrum (BIASIUCCI *et al.*, 2019). Figure

4 shows the representation of each frequency wave, including: the delta wave which is related to deep sleep or wakefulness, the theta wave is linked to a state of drowsiness such as deep meditation, the alpha wave indicates a state of relaxed consciousness, and the beta wave is related to a state of fixed attention and thought. Finally, the gamma wave with a low wave amplitude is normally used to detect brain diseases (SANEI; CHAMBERS, 2007).

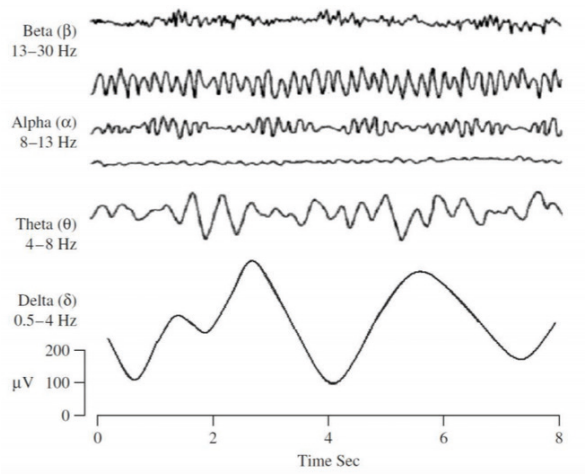

Figure 4: Image depicting frequency waves.

Source: Sanei; Chambers (2007)

Finally, the recording of the EEG signal can suffer from non-cerebral interference due to non-physiological or physiological artifacts, which can lead to behavior that is different from normal. Such as picking up signals from eye movement, muscle movement or some signal present in the environment in which it is being carried out (TATUM et al., 2008).

MATHEMATICAL TOOLS

Over the years, research into biological signals has been developed and mathematical tools are increasingly being used to understand the behavior of signals in nature. Science seeks to determine the pattern of the biological signal, but computational techniques are needed to analyze the signal in the time and frequency domain and understand its peculiarities.

Among the most widespread tools is the Fourier Transform (FT) technique, which allows a signal in the time domain to be represented as a signal in the frequency domain, so that the decomposition into frequencies makes up the original signal. In this way, any one- or two-dimensional signal can be described by the sum of sine and cosine oscillations. The TF mathematical equation is an integral transform that expresses several frequencies contained in a time series (1.1)(SILVA, 2014).

$$\boldsymbol{F(\omega) = \int_{x=-\infty}^{\infty} f(x) e^{-2\pi\omega x} dx} \qquad (1.1)$$

In which $\boldsymbol{f(x)}$ represents the analyzed time series, and the presence of the exponential indicates the transformation to the frequency domain. However, TF has a limitation when it comes to identifying the time of a signal divided into several frequencies, as non-stationary series are difficult to apply in TF (SILVA, 2014).

To remedy this deficiency, there is the *Short Time Fourier Transform* (STFT) method**,** which segregates the time series into fixed instants and calculates the time of the signal. $\boldsymbol{f(\omega)}$ in each part of the fixed periods, but depending on the size of the signal segmentation window, information may be lost. However, this technique helps to analyze non-stationary time series (SILVA, 2014).

The article by Fadzal *et al.* (2012) used the STFT method to analyze the EEG signal in the relaxed and writing conditions. The results obtained, shown in the spectrogram of the EEG signals, range from 11 to 28.38 Hz when the individual is writing and 8 to 12.25 Hz in the relaxed condition, i.e. it was possible to obtain time and frequency information with a fixed time window.

Peng *et al.* (2022) also used the STFT technique to extract features in the frequency and time domain, combined with the maximum mean discrepancy *autoencoder* technique to map the EEG signal in space. The purpose of the work was to predict epileptic

seizures. The result was 76 % sensitivity for intracranial samples of the EEG signal and 73 % for extracranial.

Arrais Junior (2016) used the Discrete Wavelet Transform Redundant (TWDR) technique from the *Daubechies* family and the *Daubechies* 4 (db4) mother *wavelet* to analyze electrocardiogram signals. The paper presented a system for analyzing electrocardiogram signals in real time using *thresholding* techniques. The system achieved sensitivity of 99.20% and positive predictivity of 99.64%.

Cortés (2021) in his final paper used the Discrete Wavelet Transform (DWT) to develop a classifier for ADHD with the *Daubechies* family and the db4 mother *wavelet*, due to the identification of unique characteristics in electrophysiological signals. In addition, the technique used to study the possible presence of ADHD was logistic regression. The performance of the classifier was 96 % for cross-validation, for a study group of 64 children

Another *wavelet* tool is the Wavelet Packet Transform, which was applied in the article by Yuan *et al.* (2017) to detect seizures in the continuous recording of the EEG signal. The algorithm's event-based sensitivity was 97.73 %. As a result, the method showed promise for assessing seizure events.

The mathematical tool used in this work was the TWDR because it has a simpler implementation from a numerical point of view, does not have subsampling by 2 and has been used over the years to analyze biomedical signals. The basis of the *wavelet* used in this work was the *Daubechies* family of type db4. In view of the work of Jahankhani, Kodogiannis and Revett (2006) who used the db4 due to its smoothing characteristic, it is useful for detecting changes in the EEG signal, as well as providing a good signal output. The same applies to Cortés (2021), who also used db4 to identify unique characteristics in electrophysiological signals.

DISCRETE WAVELET TRANSFORM

But although the STFT has contributed to the analysis of non-stationary time series, there are still some gaps, such as:

- The fixed interval (window) could not be changed;
- For trigonometric functions, the energy is infinite.

These questions gave rise to the Wavelet Transform (WT), which is a finite-energy mathematical tool that can be dilated or compressed in time, removing the fixed windowing of the STFT method (SILVA, 2014).

The TW method allows data to be analyzed at varying scales and resolutions, both globally and in terms of signal detail, thus eliminating gaps in the TF time window. TW uses various bases, including: Morlet, Biorthogonal, Mexican, Hat, Harr, Daubechies, among others, with their own characteristics. They are used in specific analyses and are displayed by the *psi* (ψ) *mother wavelet (*BARBOSA et.al, 2008).

To examine discrete signals, the multiresolution analysis mechanism allows the signal to be decomposed into approximation coefficients and *wavelet* coefficients at different scale levels and using high-pass and low-pass filters (MALLAT, 1989). The numerical equation that obtains the fast decomposition of the TWD, to obtain the coefficients are:

$$Sj(k) = \sum_{n=-\infty}^{\infty} g(n-2k)Sj-1(n) \quad (1.2)$$

$$\omega j(k) = \sum_{n=-\infty}^{\infty} h(n-2k)Sj-1(n) \quad (1.3)$$

Sj being the approximation coefficients, ωj *wavelet* coefficients, *j* resolution scale and g(k) low-pass and h(k) high-pass filters (ARRAIS JUNIOR, 2016).

The frequency spectrum of the approximation coefficients and *wavelet* coefficients at each scale *j* is given according to the sampling frequency *fs* in the range of:

$$\left[0, \frac{fs}{2^{j+1}}\right], \left[\frac{fs}{2^{j+1}}, \frac{fs}{2^{j}}\right] \quad (1.4)$$

The *mother wavelet* of the four-coefficient *Daubechies* family. The db4 has four filter coefficients for the *g* approximation coefficients, as well as four coefficients for the *h wavelet* filter (ARRAIS JUNIOR, 2016). Below are the filter coefficients.

$$g(0) = \frac{1+\sqrt{3}}{4\sqrt{2}}, g(1) = \frac{3+\sqrt{3}}{4\sqrt{2}}, g(2) = \frac{3-\sqrt{3}}{4\sqrt{2}}, g(3) = \frac{1-\sqrt{3}}{4\sqrt{2}}$$
$$h(0) = \frac{1-\sqrt{3}}{4\sqrt{2}}, h(1) = \frac{-3+\sqrt{3}}{4\sqrt{2}}, h(2) = \frac{3+\sqrt{3}}{4\sqrt{2}}, h(3) = \frac{-1-\sqrt{3}}{4\sqrt{2}}$$

REDUNDANT DISCRETE WAVELET TRANSFORM

Due to the fact that TWD uses a sub-sampling procedure for the approximation and *wavelet* coefficients because of their time-varying behavior, the efficiency of the method is impaired. As a result, we have the TWDR, which does not include the process of sub-sampling the coefficients, because it is time-invariant and allows for real-time analysis. Therefore, the TWDR equation is similar to the TWD, but without subsampling by two (PERCIVAL D. B.; WALDEN, 2000).

The equations for the approximation and *wavelet* coefficients are:

$$Sj(k) = \sum_{n=-\infty}^{\infty} \tilde{g}(n-k)Sj-1(n) \quad (1.5)$$

$$\omega j(k) = \sum_{n-\infty}^{\infty} \tilde{h}(n-k)Sj-1(n) \quad (1.6)$$

Figure 5 shows two levels of resolution of the TWDR decomposition of the input signal, which will output the approximation coefficients *s* and *wavelet* coefficients ω. With each decomposition of the signal, the approximation coefficient is used at a new scale in the process. In this way, the TWDR generalization process takes place.

The four filter coefficients for the scalar coefficients *g* and for the *wavelet* filter coefficients *h of* the TWDR are given by:

$$\tilde{g}(0) = \frac{1+\sqrt{3}}{8}, \tilde{g}(1) = \frac{3+\sqrt{3}}{8}, \tilde{g}(2) = \frac{3-\sqrt{3}}{8}, \tilde{g}(3) = \frac{1-\sqrt{3}}{8},$$
$$\tilde{h}(0) = \tilde{g}(3), \tilde{h}(1) = -\tilde{g}(2), \tilde{h}(2) = \tilde{g}(1), \tilde{h}(3) = -\tilde{g}(0)$$

From the approximation and *wavelet* coefficients it is possible to calculate the energies of the terms based on Parseval's theory (BURRUS; GOPINATH; GUO,1997).

$$\sum_{k=1}^{kt} |x(k)|^2 = \sum_{k=1}^{kt} |sj(k)|^2 + \sum_{j=1}^{J} \sum_{k=1}^{kt} |\omega j(k)|^2$$

$\sum_{k=1}^{kt} |x(k)|^2$ = Energy associated with the input signal;

$\sum_{k=1}^{kt} |sj(k)|^2$ = Energy of the *jth* scale approximation coefficients;

$\sum_{j=1}^{J} \sum_{k=1}^{kt} |\omega j(k)|^2$ = Energy of the *wavelet* coefficients of scale *j*.

PROPOSED METHOD

Based on the state of the art, studies point to increased amplitude in low-frequency bands (delta and theta) in children with ADHD, so the *wavelet* coefficients of scale 4, 5 and 6 were the points of interest since from level 4 there is already a transition to high frequencies.

Figure 6 shows the flowchart for identifying EEG signals that may be related to ADHD in children. The logic applied was empirical. Based on observations of the signal's characteristics obtained with the TWDR mathematical tool, the input EEG signal was decomposed into approximation and *wavelet* coefficients, and the energy associated with the *wavelet* coefficients was calculated at 6 levels of resolution. So, the empirical logic aims to obtain better accuracy for the set to determine signs suggestive of ADHD.

In view of the analysis logic in Figure 6, the EEG signal from children with and without ADHD was first applied to the TWDR algorithm. Next, the signal was decomposed into approximation and *wavelet* coefficients, and the energy amplitude of the *wavelet* coefficients in 6 frequency scales was presented

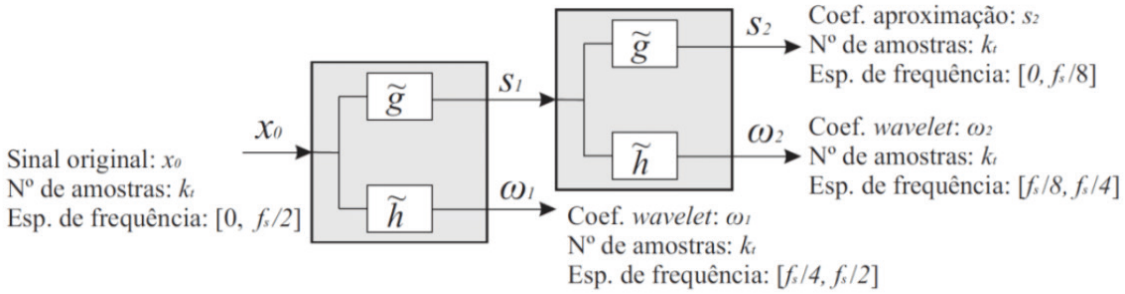

Figure 5: Two levels of TWDR resolution.

Source: Arrais Junior (2016).

in the 3 results obtained. Subsequently, the response of the *wavelet* coefficients is used as a parameter in the *threshold* technique, which evaluates the following reasoning: if the modulus of the maximum value of the wavelet coefficient of scale 6 is greater than the modulus of the maximum value of the wavelet coefficient of scale 4, and if the modulus of the maximum value of the wavelet coefficient of scale 5 is greater than the modulus of the maximum value of the wavelet coefficient of scale 4, if true, the classification will be the possible presence of ADHD. Otherwise, the algorithm classifies the individual as not having ADHD.

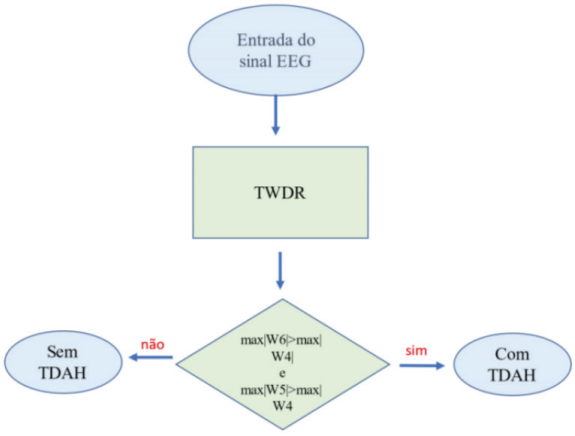

Figure 6: Flowchart for ADHD classification.

Source: Prepared by the author (2022).

DATABASE

The EEG databases for children with ADHD and without ADHD are from the *IEEE Dataport*, with free access to the data. The EEG records were obtained from medical records at the psychiatric clinic of Roozbeh Hospital in Iran. As a result, the file contains documentation on 121 patients, 61 of whom were children with ADHD and 60 without ADHD aged between 7 and 12 who had been taking ritalin for up to 6 months.

The recording of brain activity followed the 10-20 pattern, with 19 electrodes, as seen in Figure 3. The activity developed by the patients was visual attention to count the number of figures of the characters. The sampling frequency was 128 Hz and the electrode impedance was 5 kΩ. The recording time for individuals with ADHD was 285 seconds and for those without ADHD 50 seconds.

RESOLUTION LEVELS

This stage consists of breaking down the signal into scale levels. Thus, the signal acquired from the *IEEE Dataport* database has a sampling frequency of 128 Hz. However, in order to decompose the signal into 6 TWDR resolution levels, it was necessary to sample the signal at 270 Hz. The purpose of resampling was to separate the lower delta (2.1093 - 4.2187 Hz) and theta (4.2187 - 8.4375 Hz) frequencies and analyze the behavior of these frequency ranges, as can be seen in Table 2.

Scale	Frequency range [Hz]
1	67,5 - 135
2	33,75 - 67,5
3	16,875 - 33,75
4	8,4375 - 16,875
5	4,2187 - 8,4375
6	2,1093 - 4,2187

Table 2 - TWDR resolution levels

Source: Prepared by the author (2022).

CLASSIFICATION

THRESHOLD

The *threshold* values were based on the peaks of the *wavelet* coefficients at resolution level 4 (8.4375 - 16.875 Hz), 5 (4.2187 - 8.4375 Hz) and 6 (2.1093 - 4.2187 Hz). The empirical logic involves obeying the following criterion:

$$\boldsymbol{threshold = |W6|\ \ maior |W4|}$$
$$\boldsymbol{e |W5|\ maior\ max\ |W4|}$$

- The modulus of the maximum value of the wavelet coefficient of scale 6 is greater than the modulus of the maximum value of the wavelet coefficient of scale 4;
- The modulus of the maximum value of the wavelet coefficient of scale 5 is greater than the modulus of the maximum value of the wavelet coefficient of scale 4;
- If it meets the two previous criteria, it would indicate the possible presence of ADHD;
- Otherwise, the algorithm classifies them as not having ADHD.

ANALYSIS METRICS

Two parameters were used to assess the classifier's performance: Sensitivity (*Se*) and Positive Predictivity () (KOHLER; HENNIG; ORGLMEISTER, 2002), (MARTINEZ et al., 2004). In this way, the number of False Positives (FP), False Negatives (FN) and Correct Detections (CD) of the classifier is verified.

$$Se = \frac{DC}{DC+FN} \times 100$$

$$P^{+} = \frac{DC}{DC+FP} \times 100$$

Sensitivity is the probability of the algorithm detecting sick individuals. Positive predictivity, on the other hand, is the probability of the algorithm correctly identifying the existence of the disease (SOPELETE, 2005).

RESULTS AND DISCUSSIONS

Analysis of the EEG signal related to signs suggestive of ADHD is carried out using the TWDR technique. The characteristics of the decomposed signal include: Approximation coefficients resulting from the low-pass filter that attenuates high frequencies, *wavelet* coefficients resulting from the high-pass filter that attenuates low frequencies, being sensitive to large signal variations. The characteristics extracted by the TWDR tool were for the 6 levels of resolution, as shown in Table 2. Finally, the energy of the *wavelet* coefficients was also analyzed for EEG signal analysis, as shown in Table 2.

Thus, the data set analyzed consisted of 40 patients, 20 children with ADHD and 20 without ADHD from the *IEEE Dataport* database. In addition, only the frontal electrodes (Fz, Fp1, Fp2, F3, F4, F7, F8) shown in Figure 4 were analyzed, i.e. 7 of the 19 electrodes, as this region shows disparity among patients with the disorder, in addition to presenting good classification results, as presented in the state of the art.

The aim of this method is to detect possible alterations in the EEG signal indicative of ADHD in groups of children with and without ADHD. In this way, this work evaluates which scales showed discrepancies in amplitudes, either in the value of the approximation and wavelet coefficients or in the energy of the *wavelet* coefficients. To this end, 3 EEG signals were chosen from the set to demonstrate sig-

nal processing and to check for singularities. Of the three, two had ADHD and one did not have ADHD.

The following analysis shows the TWDR of the EEG signal from the v1p set of the Fz electrode, showing the recording of a patient with ADHD. In the Figures of the set, the behavior of the signal is observed and then the Figures are enlarged for the instant of interest. Figure 7a shows the EEG signal with amplitude peaks at various time points between 0 and 250 seconds. Figure 7b shows in red the moment with the highest amplitude value, around 4000 mV. This moment is a possible indication of when the child with ADHD was visually stimulated with the figures of the characters to record the EEG signal, according to the *IEEE Dataport* database. Figure 7c shows the interval of 30 to 40 seconds from the moment of greatest amplitude of the signal in Figure 7b.

Figure 8 shows the approximation coefficients for the six resolution levels using the low-pass filtering process in which high-frequency noise is attenuated from the EEG signal in Figure 7a. Based on this, Figure 8a shows the approximation coefficients in the 0 to 250 second range. Figure 8b shows the coefficients in the 30 to 40 second range with similar behavior to the original signal, however, a delay is shown as the scale increases, due to the delay being in the order of 2^j, with j indicating the level of resolution.

Figure 9a shows the *wavelet* coefficients with the 6 frequency scales in the range 0 to 250 seconds. The *wavelet* coefficients are the result of filtering the EEG signal in Figure 7a using a high-pass filter which attenuates the low noise frequencies and also captures the high variations in the EEG signal. Figure 9b shows the amplitude of the coefficients in the time interval between 30 and 40 seconds. It can be seen that W4v (8.4375 - 16.875 Hz) has a maximum amplitude value close to 1500 mV, while W5v (4.2187 - 8.4375 Hz) also has an amplitude close to 1500 mV. W6v (2.1093 - 4.2187 Hz) shows an amplitude value above -1500 mV. Therefore, the statements made by researchers Ibrahim et al. (2019) and Ekhlasi et al. (2021) were observed in this analysis, in which there was an increase in low frequencies in W6v (delta wave) and W5v (theta wave) for children with ADHD.

Finally, Figure 10a shows the energy concentrations of the *wavelet* coefficients of the signal in Figure 9a. In Figure 10b, the time domain interval has been reduced to analyze the energy concentration between 30 and 40 seconds, due to the amplitude peak that occurs in this time interval, as seen in Figure 7b.

The concentration of energy occurs on the E2 (W2v) and E3 (W3v) scales in 34 seconds, exhibiting an order of magnitude of . At another point, the concentration of energy in the *wavelet* coefficients is for scales E2 (W2v), E3 (W3v) and E4 (W4v). In contrast to Figure 9b, which showed higher amplitudes at low frequencies (W6v and W5v), the concentration of energy occurred at high frequencies.

The following analysis shows the TWDR of the EEG signal from the v18p set of electrode F7, showing the recording of a patient with ADHD. The Figures show the behavior of the signal and then zoom in to the instant of interest. Figure 11a shows the EEG signal with an amplitude peak in the interval between 0 and 250 seconds. Figure 11b shows in red the moment with the highest amplitude value above 4000 mV. This moment is a possible indication of when the child with ADHD was visually stimulated with the figures of the characters to record the EEG signal, according to the *IEEE Dataport* database. Figure 11c shows the interval of 12 to 18 seconds from the moment of greatest amplitude of the signal in Figure 11b.

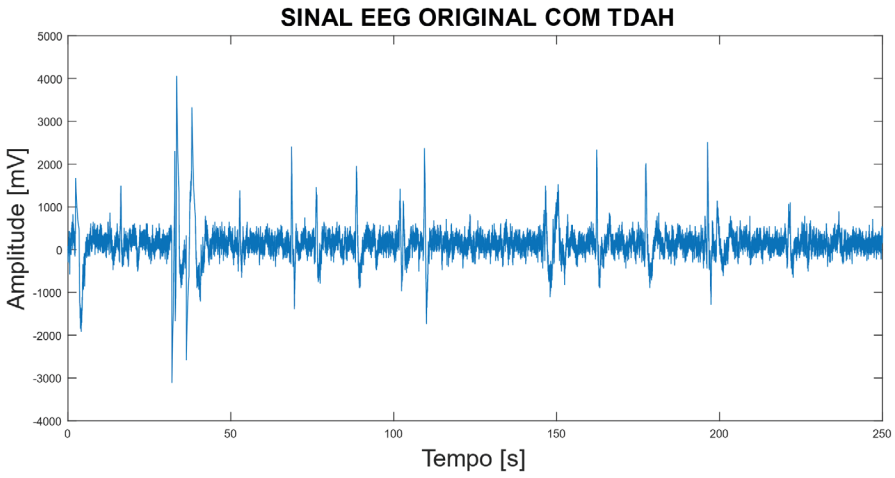

(a)

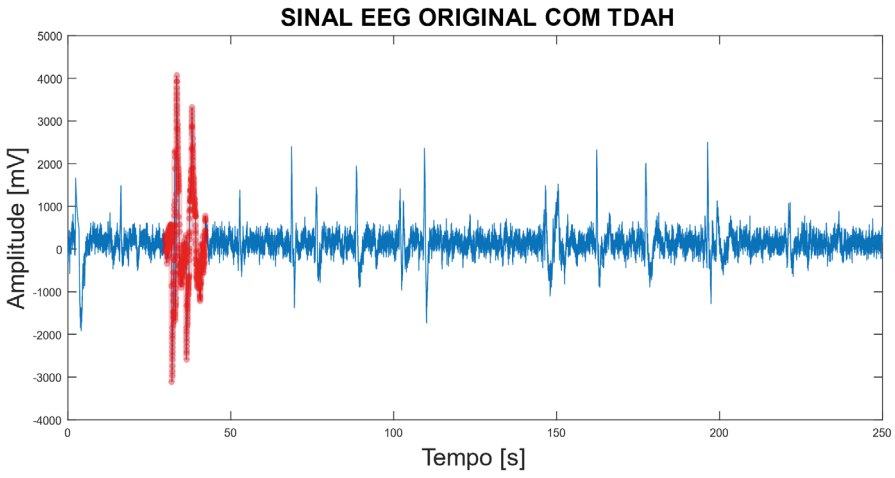

(b)

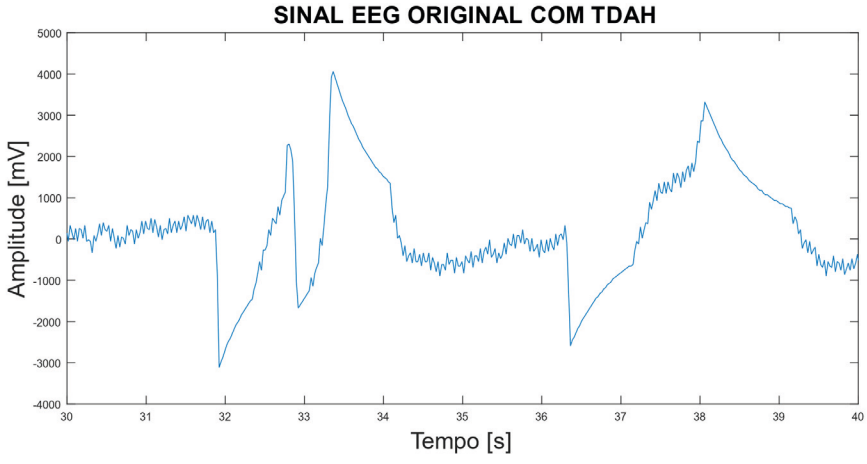

(c)

Figure 7: Signal from electrode Fz of set v1p (IEEE database), with ADHD: (a) Original signal, (b) Instant of greatest amplitude and (c) Time interval of greatest amplitude between 30 and 40s.

Source: Prepared by the author (2022).

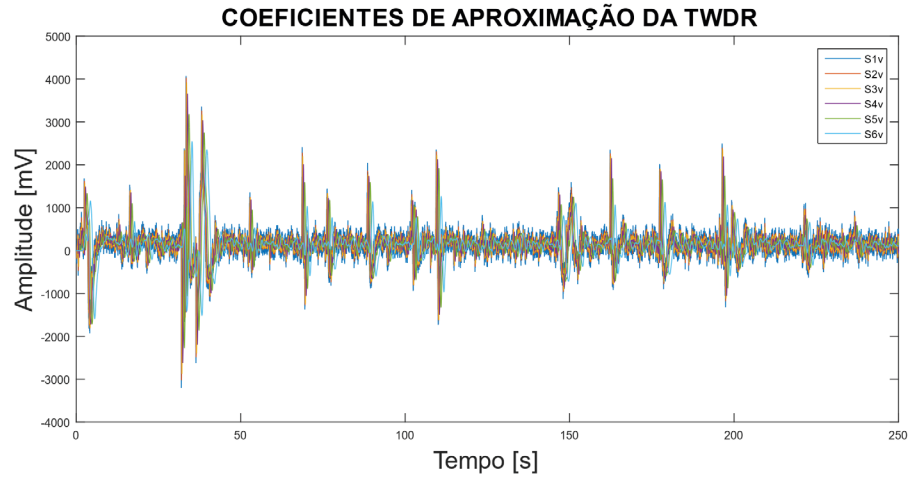

(a)

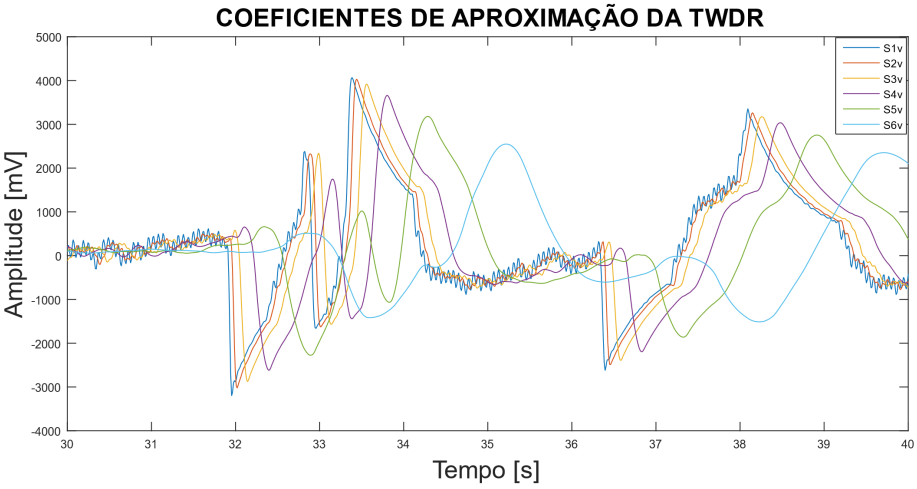

(b)

Figure 8: Fz electrode signal from the v1p set (IEEE database), with ADHF: (a)Approximation coefficients and (b)Approximation coefficients in the 30 to 40s interval.

Source: Prepared by the author (2022).

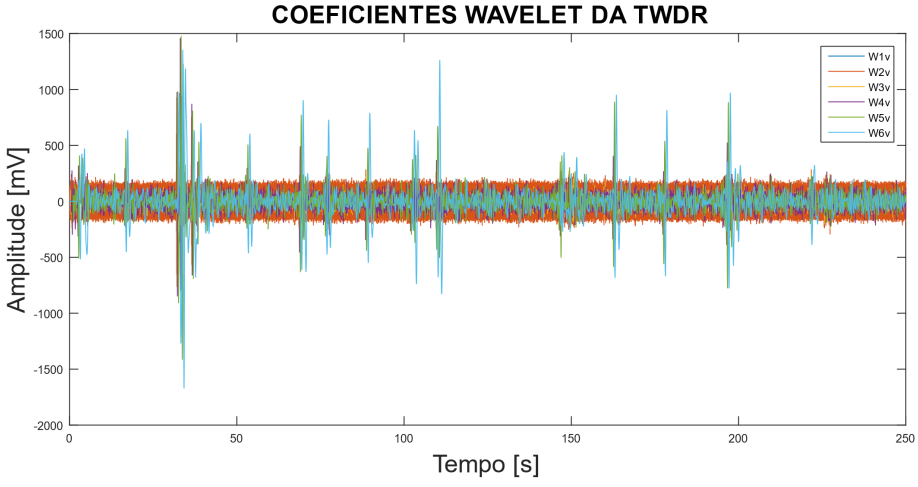

(a)

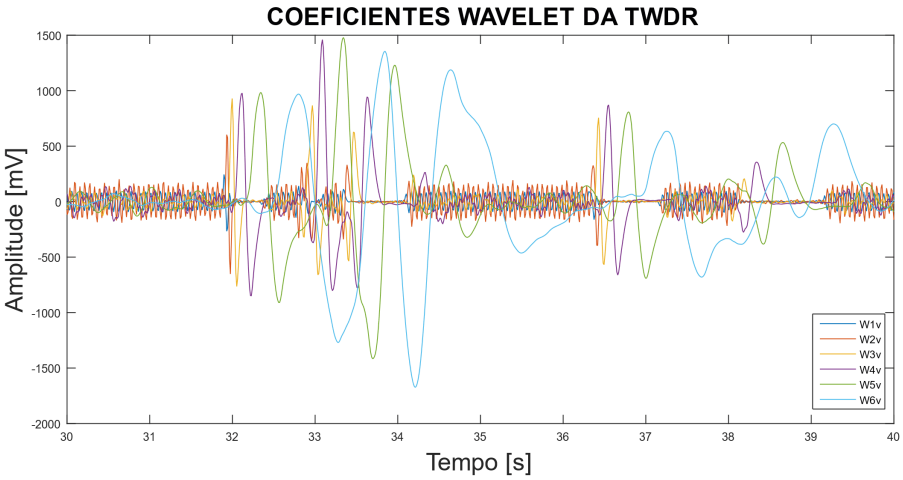

(b)

Figure 9: Fz electrode signal from the v1p set (IEEE database), with ADHD: (a)Wavelet coefficients, (b) Wavelet coefficients in the 30 to 40s interval.

Source: Prepared by the author (2022).

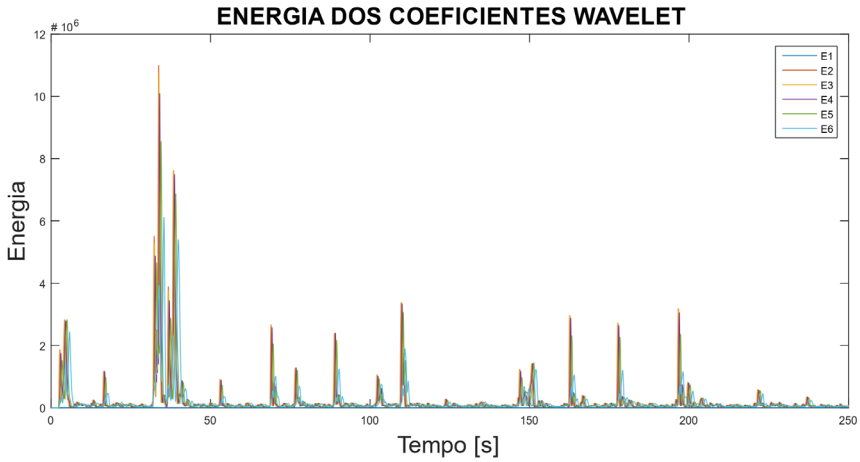

(a)

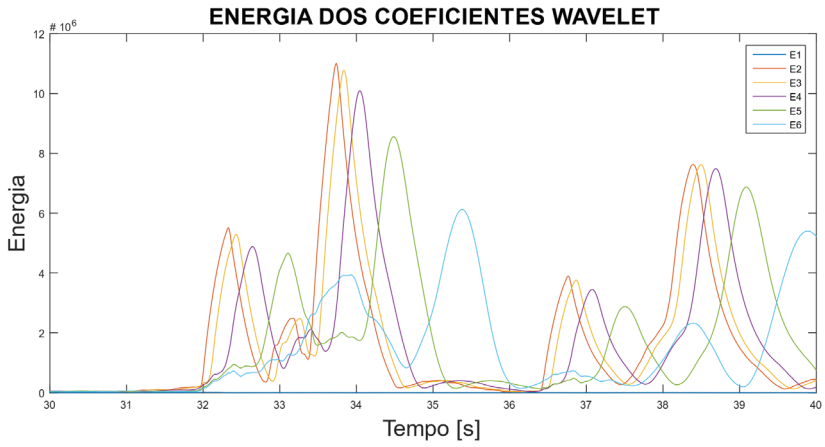

(b)

Figure 10: Fz electrode signal from the v1p set (IEEE database), with ADHD: (a) Energy of the *wavelet* coefficients and (b) Energy of the *wavelet* coefficients in the interval between 30 and 40s.

Source: Prepared by the author (2022).

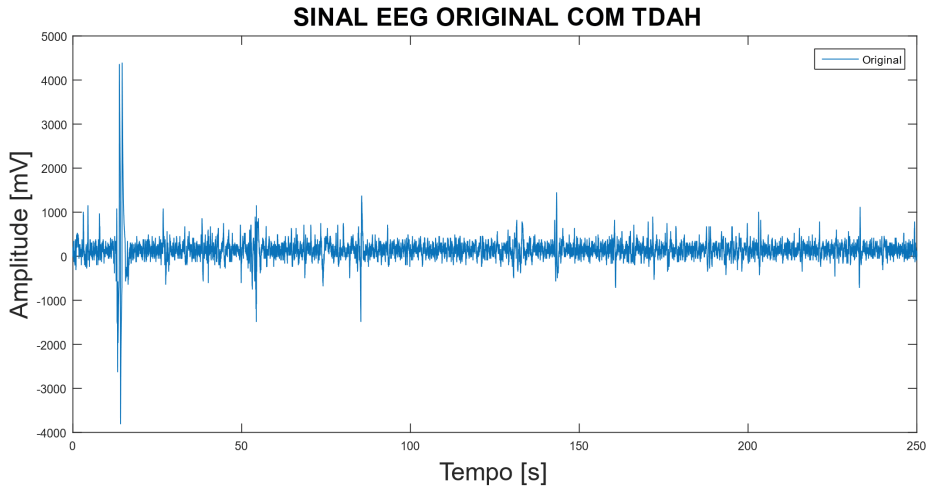

(a)

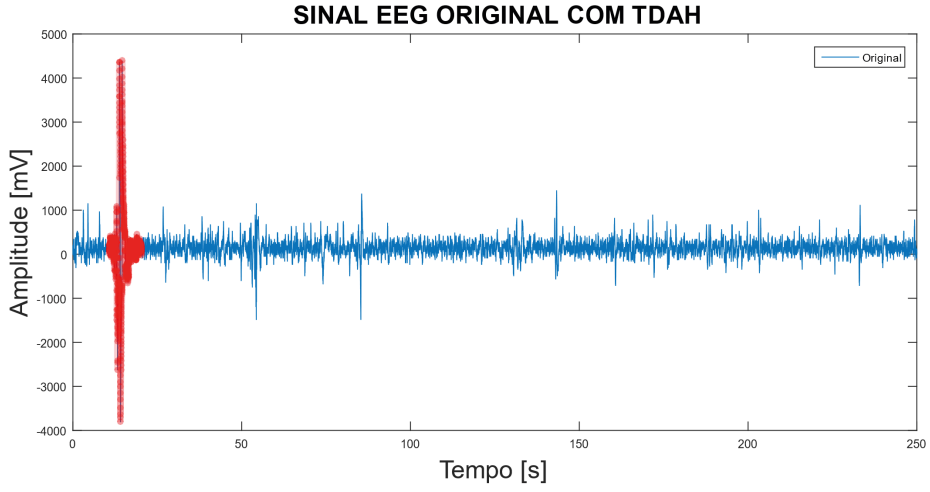

(b)

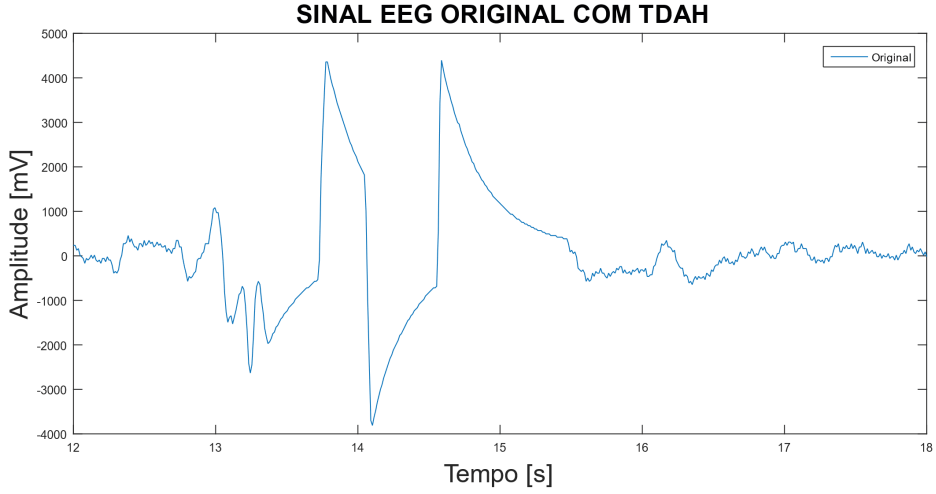

(c)

Figure 11: Signal from electrode F7 of the v18p set (IEEE database), with ADHD: (a) Original signal, (b) Instant of greatest amplitude and (c) Time interval of greatest amplitude between 12 and 18s.

Source: Prepared by the author (2022).

Figure 12 shows the approximation coefficients for the six resolution levels using the low-pass filtering process in which high-frequency noise is attenuated from the EEG signal in Figure 11a. Based on this, Figure 12a shows the approximation coefficients in the 0 to 250 second range. Figure 12b shows the coefficients in the interval from 12 to 18 seconds with similar behavior to the original signal, however, a delay is shown as the scale increases, due to the delay being in the order of 2^j, with *j* indicating the level of resolution.

Figure 13a shows the *wavelet* coefficients with the 6 frequency scales in the range from 0 to 250 seconds. The *wavelet* coefficients are the result of filtering the EEG signal in Figure 11a using a high-pass filter which attenuates the low noise frequencies and also captures the high variations in the EEG signal. Figure 13b shows the amplitude of the coefficients in the time interval between 12 and 18 seconds. It can be seen that W6v (2.1093 - 4.2187 Hz) has an amplitude value of over 2000 mV. On the other hand, W4v (8.4375 - 16.875 Hz) and W5v (4.2187 - 8.4375 Hz) have amplitude values close to 1500 mV. Therefore, the discrepancy in the low frequency in W6v (delta wave) can be observed, in line with the research by Ekhlasi et al. (2021).

Figure 13c shows a possible detection of variation in the EEG signal from Figure 11a, in the interval between 54 and 56 seconds, at W3v (16.875 - 33.75 Hz) with an amplitude value of 1000 mV.

Finally, Figure 14a shows the energy concentrations of the *wavelet* coefficients of the signal in Figure 13a. In Figure 14b, the time domain interval has been reduced to analyze the energy concentration between 12 and 18 seconds, due to the amplitude peak that occurs in this time interval, as seen in Figure 11b. The highest concentration of energy occurs at scales E2 (W2v) , E3 (W3v) and E5 (W5v) with an order of magnitude of 10^6.

The following analysis shows the TWDR of the EEG signal from the v53p set of electrode F7, showing the recording of a patient without ADHD. In the Figures of the set, the behavior of the signal is observed and then the Figures are enlarged for the instant of interest. Figure 15a shows the EEG signal with amplitude peaks at various time points between 0 and 50 seconds. Figure 15b shows in red the moment of greatest concentration of peaks with an amplitude of around 4000 mV. This moment is a possible indication of when the child without ADHD was visually stimulated with the figures of the characters to record the EEG signal, as reported by the *IEEE Dataport* database. Figure 15c shows the interval between 22 and 26 seconds from the moment of greatest concentration of signal variation in Figure 15b.

Figure 16 shows the approximation coefficients for the six resolution levels using the low-pass filtering process in which high-frequency noise is attenuated from the EEG signal in Figure 15a. Based on this, Figure 16a shows the approximation coefficients in the 0 to 50 second range. Figure 16b shows the coefficients in the interval from 22 to 26 seconds with similar behavior to the original signal, however, a delay is shown as the scale increases, due to the delay being in the order of , with *j* indicating the level of resolution.

Figure 17a shows the *wavelet* coefficients with the 6 frequency scales in the range 0 to 50 seconds. The *wavelet* coefficients are the result of filtering the EEG signal in Figure 15a using a high-pass filter which attenuates the low noise frequencies and also captures the high variations in the EEG signal. Figure 17b shows the amplitude of the coefficients in the time interval between 22 and 26 seconds. It can be seen that W3v (16.875 - 33.75 Hz) has a maximum amplitude value of around 3000 mV, as does W4v (8.4375 - 16.875 Hz) with a peak value of 3000 mV. Therefore, the EEG signal without ADHD showed higher *wavelet* coefficient amplitudes for high frequencies in W3v and W4v.

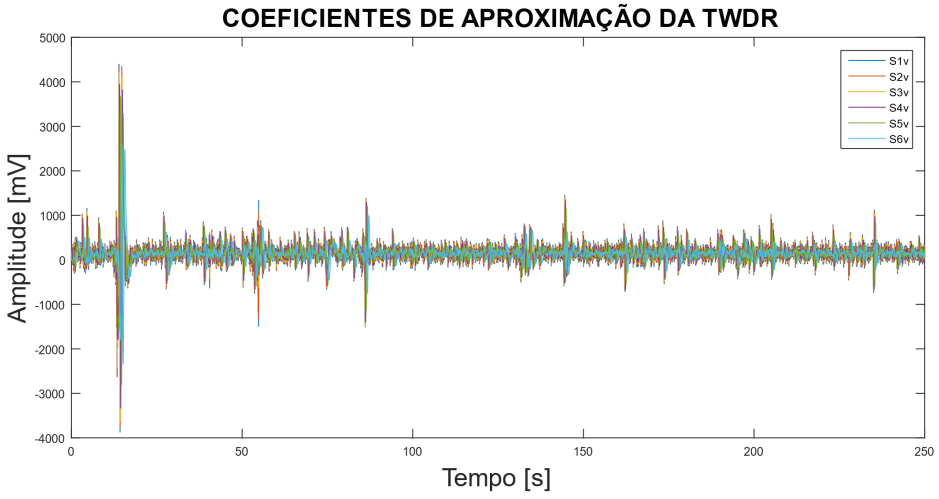

(a)

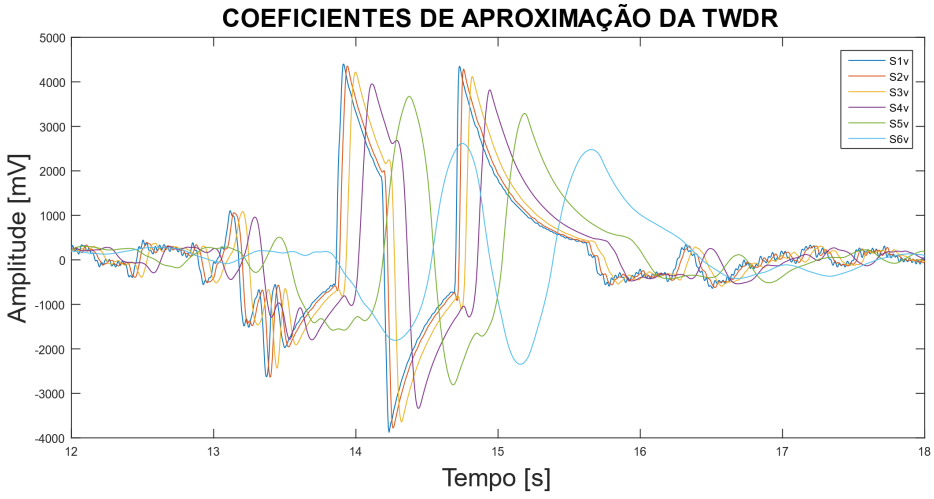

(b)

Figure 12: Signal from electrode F7 of the v18p set (IEEE database), with ADHF: (a) Approximation coefficients and (b) Approximation coefficients in the interval from 12 to 18s.

Source: Prepared by the author (2022).

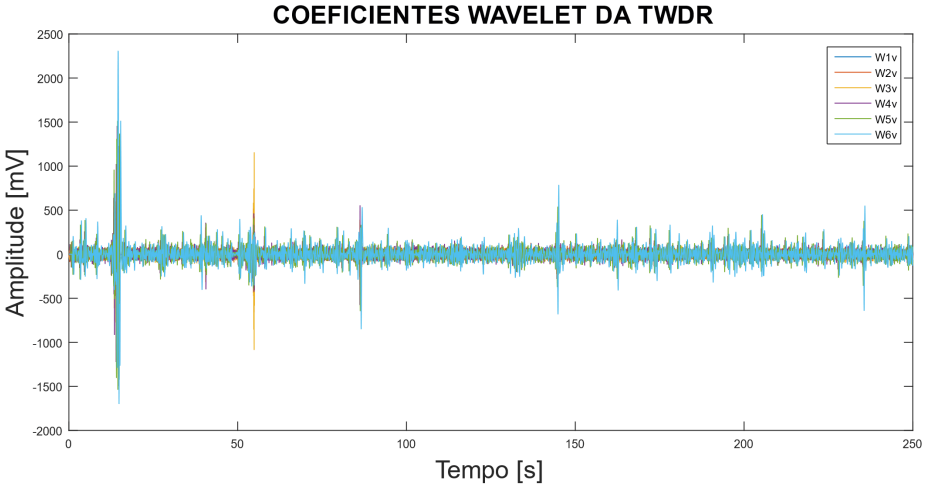

(a)

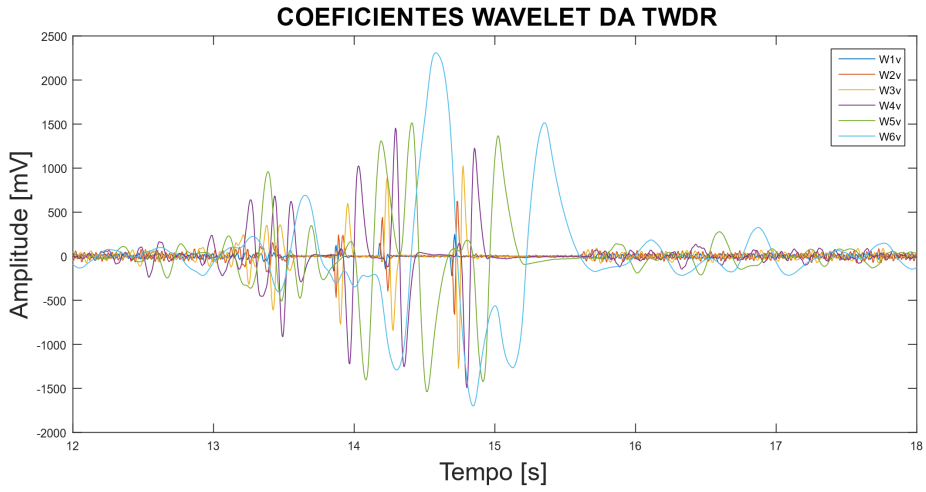

(b)

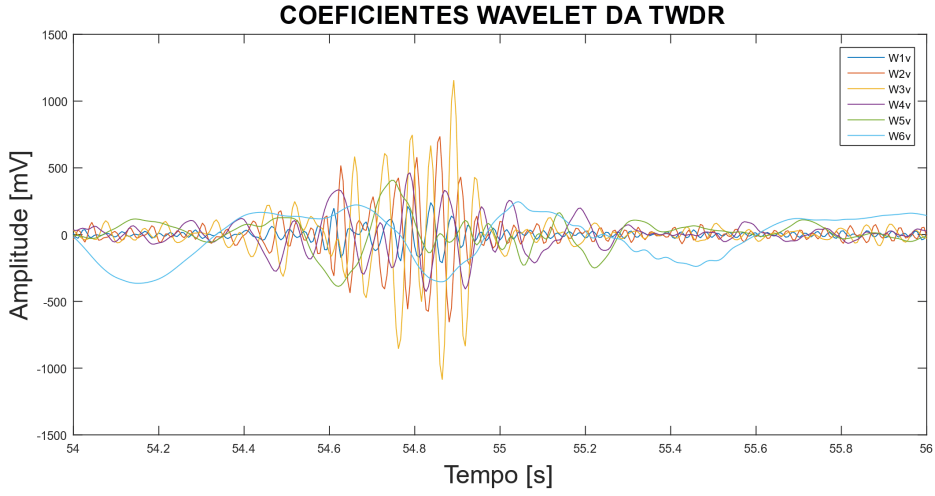

(c)

Figure 13: Signal from electrode F7 of the v18p set (IEEE database), with ADHD: (a)Wavelet coefficients, (b) Wavelet coefficients in the interval from 12 to 18s and (c) Wavelet coefficients in the interval from 54 to 56s.

Source: Prepared by the author (2022).

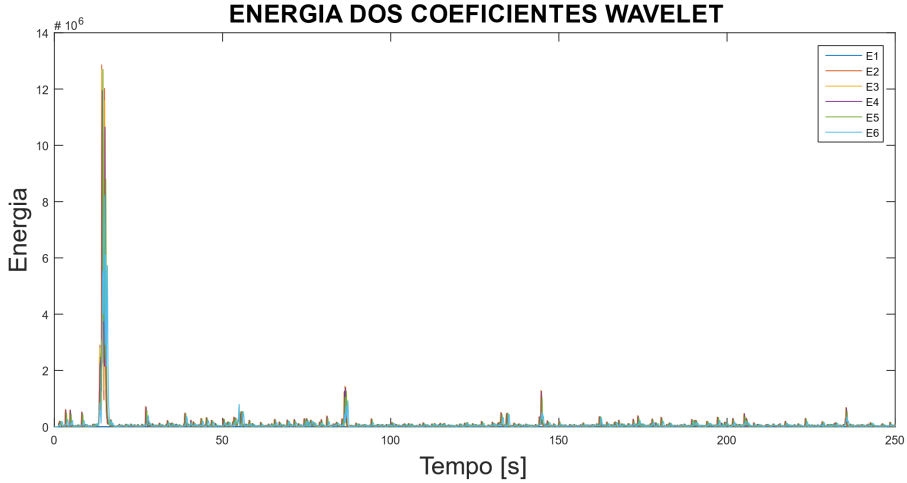

(a)

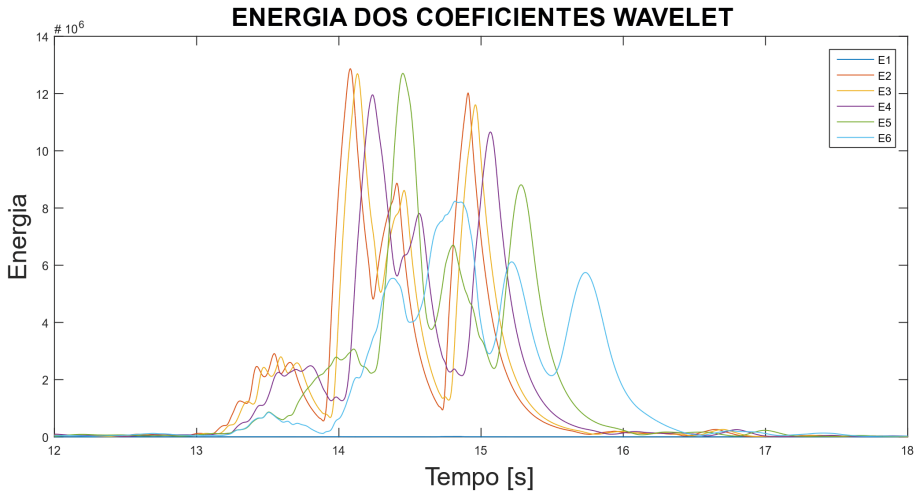

(b)

Figure 14: Signal from electrode F7 of the v18p set (IEEE database), with ADHD: (a) Energy of the *wavelet* coefficients and (b) Energy of the *wavelet* coefficients in the interval between 12 and 18s.

Source: Prepared by the author (2022).

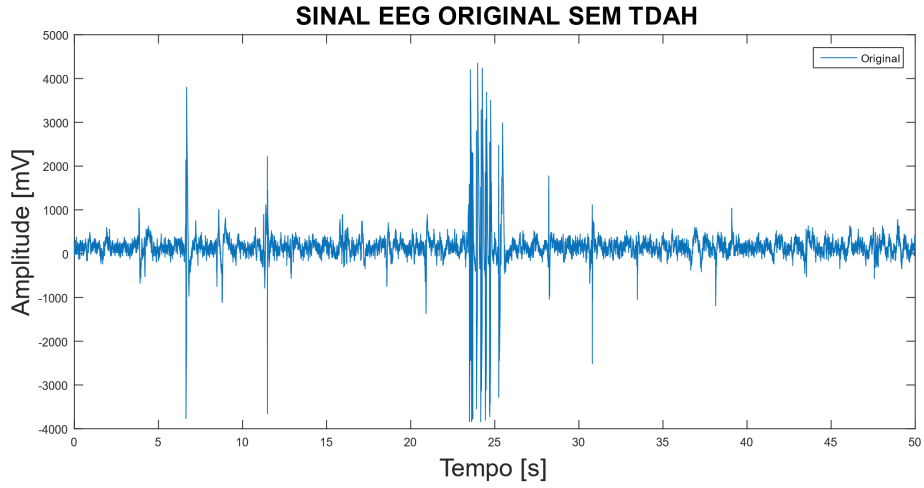

(a)

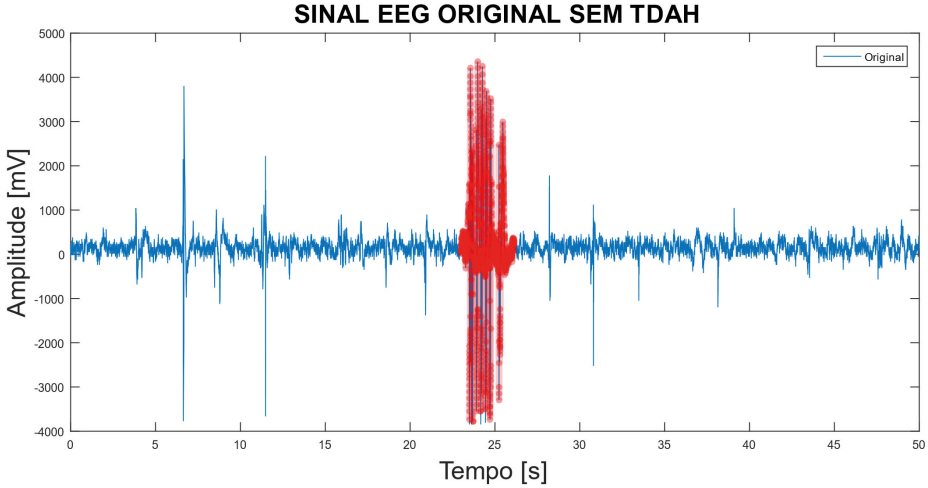

(b)

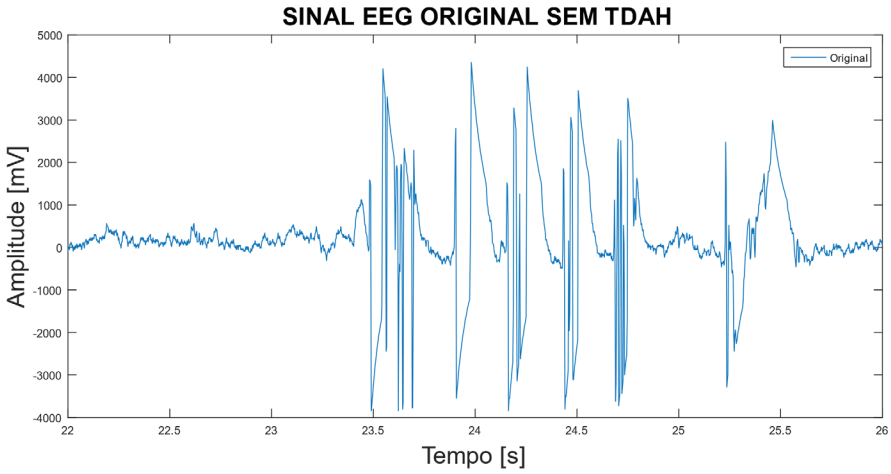

(c)

Figure 15: Figure 7: Signal from electrode F7 of the v53p set (IEEE database), without ADHD: (a) Original signal, (b) Instant of greatest amplitude and (c) Time interval of greatest amplitude between 22 and 26s.
Source: Prepared by the author (2022).

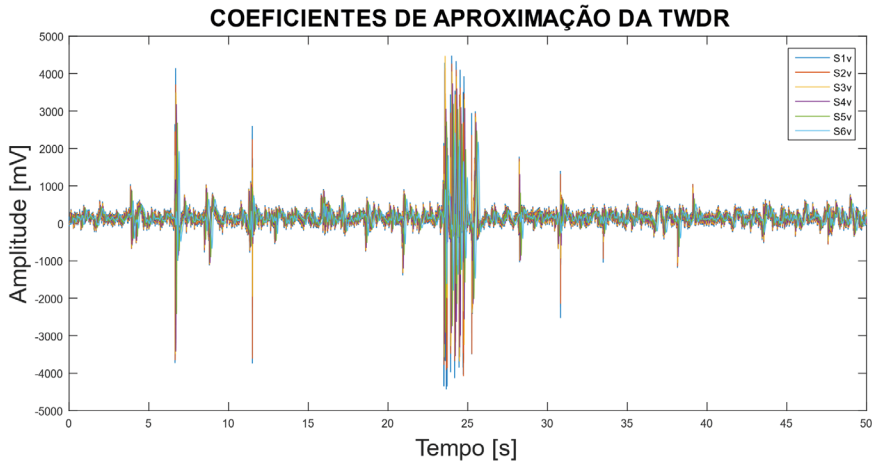

(a)

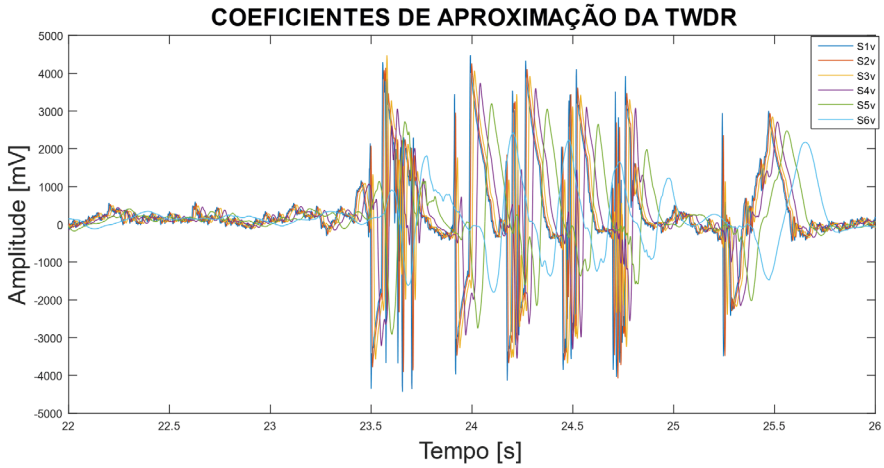

(b)

Figure 16:Figure 12: Signal from electrode F7 of the v53p set (IEEE database), without ADHF: (a) Approximation coefficients and (b)Approximation coefficients in the interval from 22 to 26s.
Source: Prepared by the author (2022).

Finally, Figure 18a shows the energy concentrations of the *wavelet* coefficients of the signal in Figure 17a. In Figure 18b, the time domain interval has been reduced to analyze the energy concentration between 22 and 26 seconds, due to the amplitude peak that occurs in this time interval, as seen in Figure 15b. The highest concentration of energy occurs on the E2 (W2v) scales with an order of magnitude of 10^6.

Finally, the energy of the *wavelet* coefficients in Figures 10b, 14b and 18b did not vary by an order of magnitude for the condition with and without ADHD. However, there is a disparity between the amplitudes of the *wavelet* coefficients between frequency ranges for Figures 9b and 13b, around W5v and W6v for those with ADHD. In contrast, Figure 17b shows an increase in the amplitude of the high-frequency coefficients W3v and W4v for the condition without ADHD.

Table 3 shows the analyses of the classifier for recognizing signs suggestive of ADHD. The data set analyzed consisted of 40 patients, 20 with ADHD (1 to 20) and 20 healthy (21 to 40). Of the 19 electrodes used to record brain activity, only 7 electrodes in the frontal region were used to test the tool. As such, the classifier performed with a sensitivity of 88.58 % and a positive predictivity of 73.26 % for the frontal electrodes.

The false positive and false negative results were significant, due to the variations in the amplitude of the *wavelet* coefficients for each electrode investigated. It was observed that the increase in amplitude in the delta and delta band did not only occur in patients with ADHD, but also in the group of patients without ADHD. Furthermore, no standard behavior was found in the EEG signal for ADHD in children, only signs suggestive of ADHD.

The results of the performance parameters were satisfactory, however, for a small volume of data. The algorithm was able to detect ADHD-related signs with a probability of 88.58 %, but for a correct classification of 73.26 % of the actual presence of ADHD.

In the process of classifying the signal, some data was disregarded because it did not show significant variation. Therefore, the result shows that the result is not highly efficient for identifying ADHD-related signals, due to the fact that it is an exploratory analysis of the data and does not analyze all the singularities of the signal. Therefore, the algorithm showed a promising result for the small group of data analyzed, favoring in-depth studies in this area of knowledge.

CONCLUSIONS

The classifier of signs suggestive of Attention-Deficit/Hyperactivity Disorder for school-age children was developed using *wavelet* coefficients (W4v, W5v and W6v) from the Redundant Discrete Wavelet Transform obtained from the EEG signal as a parameter of the *threshols* technique.

Preliminary investigations of the EEG signal with the TWDR tool showed no difference in terms of the order of magnitude of the energy of the *wavelet* coefficients in patients with ADHD and without ADHD. In addition, the amplitude of the *wavelet* coefficients showed a discrepancy for the delta and theta bands, resulting in an increase in the value of W5v and w6V in the ADHD condition, but in some groups of patients without ADHD this similarity was also observed.

The algorithm performed with *Se* = 88.58 % and 73.26 % for the frontal region of the brain. Thus, the classifier does not have a high probability of detecting signals related to the disorder due to the small number of data analyzed, only 40, with 20 patients with ADHD and 20 without ADHD. Furthermore,

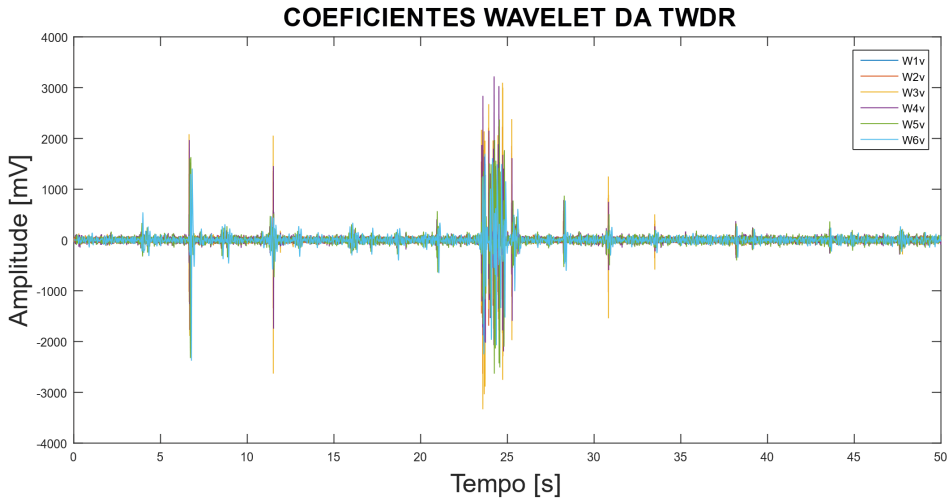

(a)

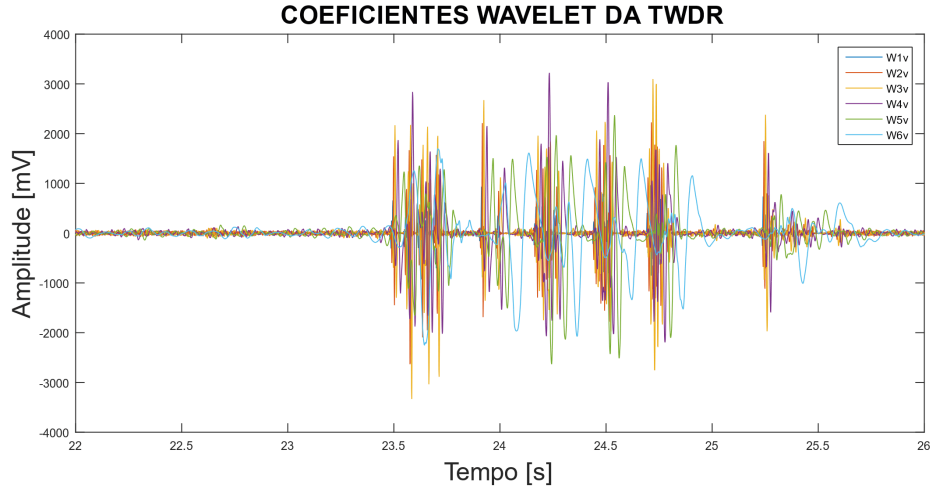

(b)

Figure 17: Signal from electrode F7 of the v53p set (IEEE database), without ADHD: (a) Wavelet coefficients and (b) Wavelet coefficients in the interval from 22 to 26s.

Source: Prepared by the author (2022).

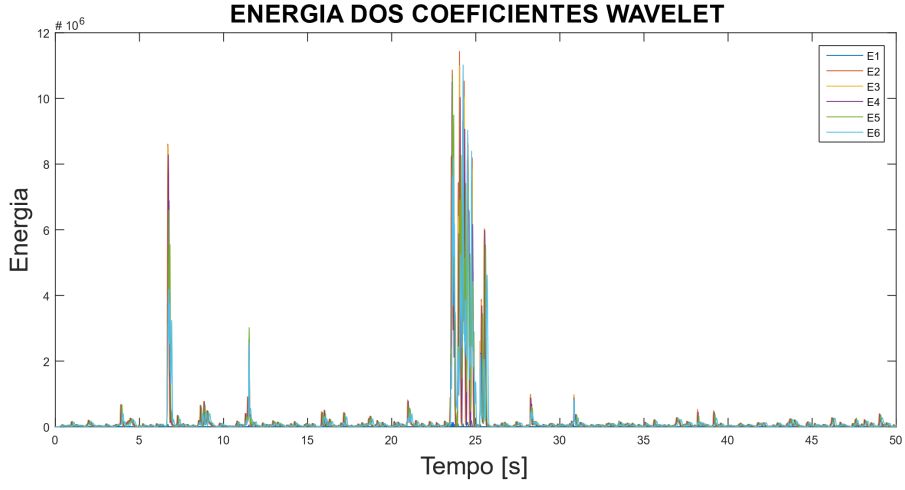

(a)

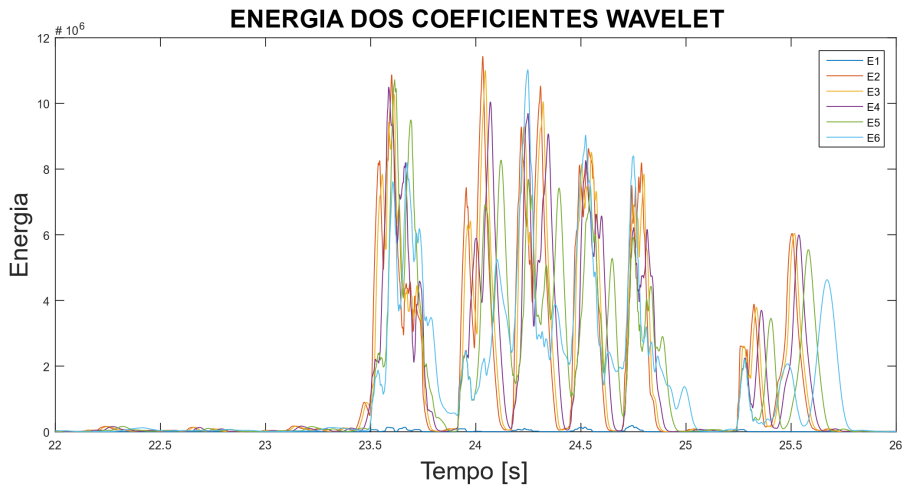

(b)

Figure 18: Signal from electrode F7 of the v53p set (IEEE database), without ADHD: (a) Energy of the wavelet coefficients and (b) Energy of the wavelet coefficients in the interval between 22 and 26s.

Source: Prepared by the author (2022).

	WAVELT PICOS	FN	FP	TOTAL FAILURES
1	49	23	0	23
2	127	6	0	6
3	20	5	0	5
4	54	6	0	6
5	54	5	0	5
6	59	5	0	5
7	98	6	0	6
8	145	4	0	4
9	97	12	0	12
10	63	3	0	3
11	147	5	0	5
12	38	0	0	0
13	6	0	0	0
14	67	7	0	7
15	66	1	0	1
16	149	0	0	0
17	63	33	0	33
18	199	195	0	195
19	23	19	0	19
20	9	0	0	0
21	19	0	14	14
22	210	0	203	203
23	28	0	23	23
24	32	0	29	29
25	40	0	37	37
26	39	0	38	38
27	42	0	36	36
28	38	0	33	33
29	40	0	38	38

30	98	0	85	85
31	36	0	36	36
32	31	0	29	29
33	30	0	5	5
34	129	0	120	120
35	34	0	31	31
36	43	0	37	37
37	35	0	31	31
38	5	0	5	5
39	53	0	43	43
40	85	0	76	76
TOTAL	2600	335	949	1284

Table 3- Table with the results for detecting signal characteristics, according to the proposed method

Source: Prepared by the author (2022).

the EEG signal does not behave in a standard way, and artifacts, whether physiological or non-physiological, also influence the acquisition of the signal, adding noise to the recorded signal.

Despite the difficulty in identifying signs related to ADHD, the results were promising, even though the work was exploratory in its analysis of signs related to ADHD in schoolchildren.

FUTURE WORK

- Perform TWDR analysis for all brain regions (Frontal, Occipital, Parietal, Temporal and Central);
- Classify the ADHD signal in all brain regions (Frontal, Occipital, Parietal, Temporal and Central);
- To carry out a statistical study on which Wavelet family has the best applicability for EEG signal analysis. Evaluating the Discrete Wavelet Transform and the Packet Wavelet Transform.

REFERENCES

9. ABDA. Associação Brasileira de Déficit de Atenção. O que é o TDAH. Disponível em: <http://www.tdah.org.br/br/sobre-tdah/o-que-e-o-tdah.html>. Acesso em: Dezembro 2022.

10. ALLAHVERDY, Armin et al. "Detecting ADHD Children using the Attention Continuity as Nonlinear Feature of EEG." (2016).

11. ALTURKI, Fahd A. *et al.* EEG Signal Analysis for Diagnosing Neurological Disorders Using Discrete Wavelet Transform and Intelligent Techniques. **Sensors**, [S.L.], v. 20, n. 9, p. 2505, 28 abr. 2020. MDPI AG. http://dx.doi.org/10.3390/s20092505.

12. American Psychiatric Association. 2014. Manual diagnóstico e estatístico de transtornos mentais: DSM-5 [Recurso eletrônico]. (5a ed.; M. I. C. Nascimento, Trad.). Porto Alegre, RS: Artmed.

13. ARRAIS JUNIOR, Ernano. **Sistema de Análise de Sinal Cardíaco para Aplicação em Telecardiologia**. 2016. 157 f. Tese (Doutorado) - Curso de Programa de Pós-Graduação em Engenharia Elétrica e de Computação, Centro de Tecnologia, Universidade Federal do Rio Grande do Norte, Natal, 2016.

14. BARBOSA et.al, 2008 Barbosa,A.C.B. (2) Blitzkow, D. Ondaletas : Histórico e Aplicação.(1) Instituto de Astronomia, Geofísica e Ciências Atmosféricas da Universidade de São Paulo – IAG/USP; (2) Escola Politécnica da Universidade de São Paulo – EPUSP – PTR – LTG. Maio, 2008.

15. BARBOSA et.al, 2008 Barbosa,A.C.B. (2) Blitzkow, D. Ondaletas : Histórico e Aplicação.(1) Instituto de Astronomia, Geofísica e Ciências Atmosféricas da Universidade de São Paulo – IAG/USP; (2) Escola Politécnica da Universidade de São Paulo – EPUSP – PTR – LTG. Maio, 2008.

16. BIASIUCCI, Andrea *et al*. Electroencephalography. **Current Biology**, [S.L.], v. 29, n. 3, p. R80-R85, fev. 2019. Elsevier BV. http://dx.doi.org/10.1016/j.cub.2018.11.052.

17. BRASIL. Ministério da Saúde. Protocolo Clínico e Diretrizes Terapêuticas do Transtorno do Déficit de Atenção com Hiperatividade. Portaria nº 14, de 29 de Julho de 2022.

18. BURRUS, C. S.; GOPINATH, R. A.; GUO, H. *Introduction to Wavelets and WaveletTransforms: A Primer*. 1. ed. [S.l.]: Prentice Hall, 1997.

19. CHEN, He *et al*. EEG characteristics of children with attention-deficit/hyperactivity disorder. **Neuroscience**, [S.L.], v. 406, p. 444-456, maio 2019. Elsevier BV. http://dx.doi.org/10.1016/j.neuroscience.2019.03.048.

20. CORTÉS, Julián D. P. **Characterization of electroencephalographic signals using discrete wavelet transform as a tool to support the diagnosis of attention deficit hyperactivity disorder ADHD**: caracterización de señales electroencefalográficas utilizando la transformada wavelet discreta como herramienta para apoyar el diagnóstico del trastorno por déficit de atención e hiperactividad tdah. 2021. 36 f. TCC (Graduação) - Curso de Electrical Engineering, Engineering Faculty - Electrical Engineering Program, Universidad Tecnológica de Pereira, Risaralda, 2021.

21. COURAS, Hirmina M. et al. Incidência de TDAH em escolares da rede pública municipal de uma cidade do alto sertão Paraibano. Revista Interdisciplinar em Saúde, Cajazeiras, 5 (2): 370-381, abr./jun. 2018, ISSN: 2358-7490.

22. DUBREUIL-VALL, L. ; RUFFINI, G.; CAMPRODON, JA.; Deep Learning Convolutional Neural Networks Discriminate Adult ADHD From Healthy Individuals on the Basis of Event-Related Spectral EEG. Front Neurosci. 2020 Apr 9;14:251. doi: 10.3389/fnins.2020.00251. PMID: 32327965; PMCID: PMC7160297.

23. EKHLASI, Ali *et al*. Direction of information flow between brain regions in ADHD and healthy children based on EEG by using directed phase transfer entropy. ***Cognitive Neurodynamics***, [S.L.], v. 15, n. 6, p. 975-986, 8 maio 2021. Springer Science and Business Media LLC. http://dx.doi.org/10.1007/s11571-021-09680-3.

24. FADZAL, C. W. N. F. Che Wan *et al*. Short-time Fourier Transform analysis of EEG signal from writing. ***2012 Ieee 8Th International Colloquium On Signal Processing And Its Applications***, [S.L.], mar. 2012. IEEE. http://dx.doi.org/10.1109/cspa.2012.6194785.

25. GIERTUGA, Katarzyna *et al*. Age-Related Changes in Resting-State EEG Activity in Attention Deficit/Hyperactivity Disorder: A Cross-Sectional Study. Front Hum Neurosci. 2017 May 30;11:285. doi: 10.3389/fnhum.2017.00285. PMID: 28620288; PMCID: PMC5451878.

26. IBRAHIM, Alaa Z. *et al*. ROLE OF ELECTROENCEPHALOGRAME IN DIAGNOSIS OF ATTENTION DEFICIT HYPER ACTIVITY DISORDER. ***Zagazig University Medical Journal***, [S.L.], v. 25, n. 3, p. 439-446, 1 maio 2019. Egypts Presidential Specialized Council for Education and Scientific Research. http://dx.doi.org/10.21608/zumj.2019.30949.

27. JAHANKHANI, Pari; KODOGIANNIS, Vassilis; REVETT, Kenneth. EEG Signal Classification Using Wavelet Feature Extraction and Neural Networks. ***Ieee John Vincent Atanasoff 2006 International Symposium On Modern Computing (Jva'06)***, [S.L.], p. 1-14, out. 2006. IEEE. http://dx.doi.org/10.1109/jva.2006.17.

28. KOHLER, B.-U.; HENNIG, C.; ORGLMEISTER, R. The principles of software qrs detection. Engineering in Medicine and Biology Magazine, IEEE, v. 21, n. 1, p. 42–57, Jan 2002. ISSN 0739-5175.

29. MALLAT, S. G. A theory for multiresolution signal decomposition: the wavelet representation. *Pattern Analysis and Machine Intelligence, IEEE Transaction*s on, v. 11, n. 7,p. 674–693, Jul 1989. ISSN 0162-8828.

30. MARKOVSKA-SIMOSKA, Silvana; POP-JORDANOVA, Nada. Quantitative EEG in Children and Adults With Attention Deficit Hyperactivity Disorder. **Clinical Eeg And Neuroscience**, [S.L.], v. 48, n. 1, p. 20-32, 10 jul. 2016. SAGE Publications. http://dx.doi.org/10.1177/1550059416643824.

31. MARTINEZ, J. *et al*. A wavelet-based EEG delineator: evaluation on standard databases. Biomedical Engineering, IEEE Transactions on, v. 51, n. 4, p. 570–581, April 2004. ISSN 0018-9294.

32. MOHAMMADI, Mohammad Reza *et al*. EEG classification of ADHD and normal children using non-linear features and neural network. ***Biomedical Engineering Letters***, [S.L.], v. 6, n. 2, p. 66-73, maio 2016. Springer Science and Business Media LLC. http://dx.doi.org/10.1007/s13534-016-0218-2.

33. Morsh, Telemediciana. MAUNUAL DE EEG PARA MÉDICOS DO TRABALHO. 2021, 17 páginas.

34. NASRABADI, Ali M. *et al*. "EEG data for ADHD / Control children"., June 10, 2020, *IEEE Dataport*, doi: https://dx.doi.org/10.21227/rzfh-zn36.

35. OLIVEIRA, Dagoberto. B. de. et al. Prevalência do transtorno de déficit de atenção e hiperatividade (TDAH) em uma Escola Pública da cidade de Salvador, BA. **Revista de Ciências Médicas e Biológicas**, *[S. l.]*, v. 15, n. 3, p. 354–358, 2016. DOI: 10.9771/cmbio.v15i3.18215. Disponível em: https://periodicos.ufba.br/index.php/cmbio/article/view/18215. Acesso em: 5 dez. 2022.

36. PEDROSO, L. et al. TRANSTORNO DO DÉFICIT DE ATENÇÃO E HIPERATIVIDADE (TDAH) INCLUSÃO ESCOLAR NAS ESCOLAS PÚBLICAS DE URUGUAIANA - RS. **Anais do Salão Internacional de Ensino, Pesquisa e Extensão**, v. 2, n. 14, 23 nov. 2022.

37. PENG, Peizhen *et al*. Seizure Prediction in EEG Signals Using STFT and Domain Adaptation. ***Frontiers In Neuroscience***, [S.L], 18 jan. 2022. Frontiers Media SA. http://dx.doi.org/10.3389/fnins.2021.825434.

38. PERCIVAL D. B.; WALDEN, A. T. Wevelet Methods for Time Series Analysis. New York, USA: Cambridge University Press, 2000

39. RAHMAN, Md. Asadur *et al*. Multiclass EEG signal classification utilizing Rényi min-entropy-based feature selection from wavelet packet transformation. **Brain Informatics**, [S.L.], v. 7, n. 1, 16 jun. 2020. Springer Science and Business Media LLC. http://dx.doi.org/10.1186/s40708-020-00108-y.

40. SANEI, S.; CHAMBERS, J. A. Eeg signal processing. Wiley Online Library, 2007.

41. SILVA, Aldo V. TRANSFORMADA WAVELETS - ABORDAGEM DE SUA APLICABILIDADE. Revista Científica Semana Acadêmica, v. 01, p. 01, 2014.

42. SLATER, Jessica *et al*. Can electroencephalography (EEG) identify ADHD subtypes? A systematic review. **Neuroscience & Biobehavioral Reviews**, [S.L.], v. 139, p. 104752, ago. 2022. Elsevier BV. http://dx.doi.org/10.1016/j.neubiorev.2022.

43. SOPELETE, Mônica C. Métodos de análise em estudos sobre diagnóstico. **Pesquisa na Área Biomédica**: do planejamento à publicação, [S.L.], v. 1, n. 1, p. 203-223, 2005. EDUFU. http://dx.doi.org/10.7476/9788570785237.0009.

44. TAGHIBEYGLOU, Behrad *et al.* Detection of ADHD cases using CNN and classical classifiers of raw EEG. ***Computer Methods And Programs In Biomedicine Update***, [S.L.], v. 2, p. 100080, 2022. Elsevier BV. http://dx.doi.org/10.1016/j.cmpbup.2022.100080.

45. TATUM, William O. et al. The Handbook of EEG Interpretation. New York: Demos Medical Publishing, 2008.

46. YUAN, Qi *et al*. Epileptic seizure detection based on imbalanced classification and wavelet packet transform. ***Seizure***, [S.L.], v. 50, p. 99-108, ago. 2017. Elsevier BV. http://dx.doi.org/10.1016/j.seizure.2017.05.018.